nature biotechnology

ARTICLES

https://doi.org/10.1038/s41587-022-01328-9

In vivo engineered B cells secrete high titers of broadly neutralizing anti-HIV antibodies in mice

Alessio D. Nahmad[1,2,8], Cicera R. Lazzarotto[3], Natalie Zelikson[4], Talia Kustin[5], Mary Tenuta[6], Deli Huang[6], Inbal Reuveni[1,2], Daniel Nataf[1,2], Yuval Raviv[1,2], Miriam Horovitz-Fried[1,2], Iris Dotan[1,2], Yaron Carmi[7], Rina Rosin-Arbesfeld[4], David Nemazee[6], James E. Voss[6], Adi Stern[5], Shengdar Q. Tsai[3] and Adi Barzel[1,2] ✉

Transplantation of B cells engineered ex vivo to secrete broadly neutralizing antibodies (bNAbs) has shown efficacy in disease models. However, clinical translation of this approach would require specialized medical centers, technically demanding protocols and major histocompatibility complex compatibility of donor cells and recipients. Here we report in vivo B cell engineering using two adeno-associated viral vectors, with one coding for *Staphylococcus aureus* Cas9 (saCas9) and the other for 3BNC117, an anti-HIV bNAb. After intravenously injecting the vectors into mice, we observe successful editing of B cells leading to memory retention and bNAb secretion at neutralizing titers of up to 6.8 μg ml^{-1}. We observed minimal clustered regularly interspaced palindromic repeats (CRISPR)–Cas9 off-target cleavage as detected by unbiased CHANGE-sequencing analysis, whereas on-target cleavage in undesired tissues is reduced by expressing saCas9 from a B cell-specific promoter. In vivo B cell engineering to express therapeutic antibodies is a safe, potent and scalable method, which may be applicable not only to infectious diseases but also in the treatment of noncommunicable conditions, such as cancer and autoimmune disease.

Broadly neutralizing antibodies (bNAbs) against HIV can suppress viremia. In particular, combination therapy with the bNAbs 3BNC117 and 10-1074 allowed long-term suppression on interruption of antiretroviral therapy in individuals with antibody-sensitive viral reservoirs[1]. Similarly, viremic individuals with dual antibody-sensitive viruses experienced diminished viremia for 3 months following the first of up to three dual-bNAb infusions[2]. However, the mean elimination half-life of the bNAbs is 16 and 23 days, respectively[3], allowing the virus to rebound. Moreover, individuals with previous resistance to one of the bNAbs have mounted resistance to the second antibody, and individuals with previous resistance to both antibodies were excluded from the trials. Limited bNAb persistence may be addressed by constitutive expression from muscle following viral vector transduction[4,5]. However, anti-drug antibodies may develop[6], possibly because of improper glycosylation. Moreover, antibodies expressed from muscle do not undergo class switch recombination (CSR) or affinity maturation, which may be required for long-term suppression of a diverse and continuously evolving HIV infection. To overcome these challenges, we[7,8] and others[9–13] have developed B cell engineering for antibody expression. In particular, we previously combined Toll-like receptor (TLR)-mediated ex vivo activation of B cells with in vivo prime-boost immunizations, and demonstrated that engineered B cells allow immunological memory, CSR, somatic hypermutation (SHM) and clonal selection. However, cost and complexity of autologous B cell engineering ex vivo may be prohibitive. At the same time, use of engineered allogeneic B cells is challenging due to the requirement for human leukocyte antigen matching for receiving T cell help and avoiding graft rejection.

These challenges may be addressed using in vivo engineering. In vivo T cell engineering was previously demonstrated, using promiscuously integrating vectors[14–21], episomal adeno-associated viral (AAV) vectors[21–24] or messenger RNA[25,26]. However, in B cells, only the specific targeting of the *IgH* locus, using the endogenous constant exons with appropriate splicing signals, is expected to allow a well regulated expression of the antibody, first as a membrane bound B cell receptor (BCR) and then, on antigen-induced activation, also as a soluble protein, released by progeny plasmablasts and plasma cells[11–13]. *IgH* targeting is similarly required for memory retention, CSR, SHM and clonal selection[7,8]. Therefore, we describe here an in vivo B cell engineering protocol based on a single systemic injection of AAV vectors coding for clustered regularly interspaced palindromic repeats (CRISPR)–Cas9 and for the desired bNAb cassette, which is targeted for integration into the *IgH* locus.

Results

Engineering strategy. To promote in vivo B cell engineering, we used a pair of AAV-DJ vectors[27], one coding for *Staphylococcus aureus* Cas9 (saCas9)[28] and the other coding for the 3BNC117 anti-HIV bNAb[29] (Fig. 1). In the first set of experiments, the saCas9 is expressed from the ubiquitously active cytomegalovirus (CMV) promoter, and the single-guide RNA, targeting saCas9 to the *IgH* locus, is coded on the same AAV. The bNAb, in turn, is coded as a bicistronic cassette under the control of an *IgH*-enhancer-dependent promoter and flanked by homology arms to the desired saCas9 cut site within the J-C intron of the *IgH* locus[7]. The bNAb cassette includes the full light chain and the variable segment of the heavy

[1]The School of Neurobiology, Biochemistry and Biophysics, The George S. Wise Faculty of Life Sciences, Tel Aviv University, Tel Aviv, Israel. [2]The Varda and Boaz Dotan Center for Advanced Therapies, The Sourasky Medical Center and Tel Aviv University, Tel Aviv, Israel. [3]Department of Hematology, St Jude Children's Research Hospital, Memphis, TN, USA. [4]Department of Clinical Microbiology and Immunology, Sackler Faculty of Medicine, Tel Aviv University, Tel Aviv, Israel. [5]The Shmunis School of Biomedicine and Cancer Research, The George S. Wise Faculty of Life Sciences, Tel Aviv University, Tel Aviv, Israel. [6]Department of Immunology and Microbiology, The Scripps Research Institute, La Jolla, CA, USA. [7]Department of Pathology, Sackler Faculty of Medicine, Tel Aviv University, Tel Aviv, Israel. [8]Present address: Tabby Therapeutics Ltd, Ness Ziona, Israel. ✉e-mail: adibarzel@tauex.tau.ac.il

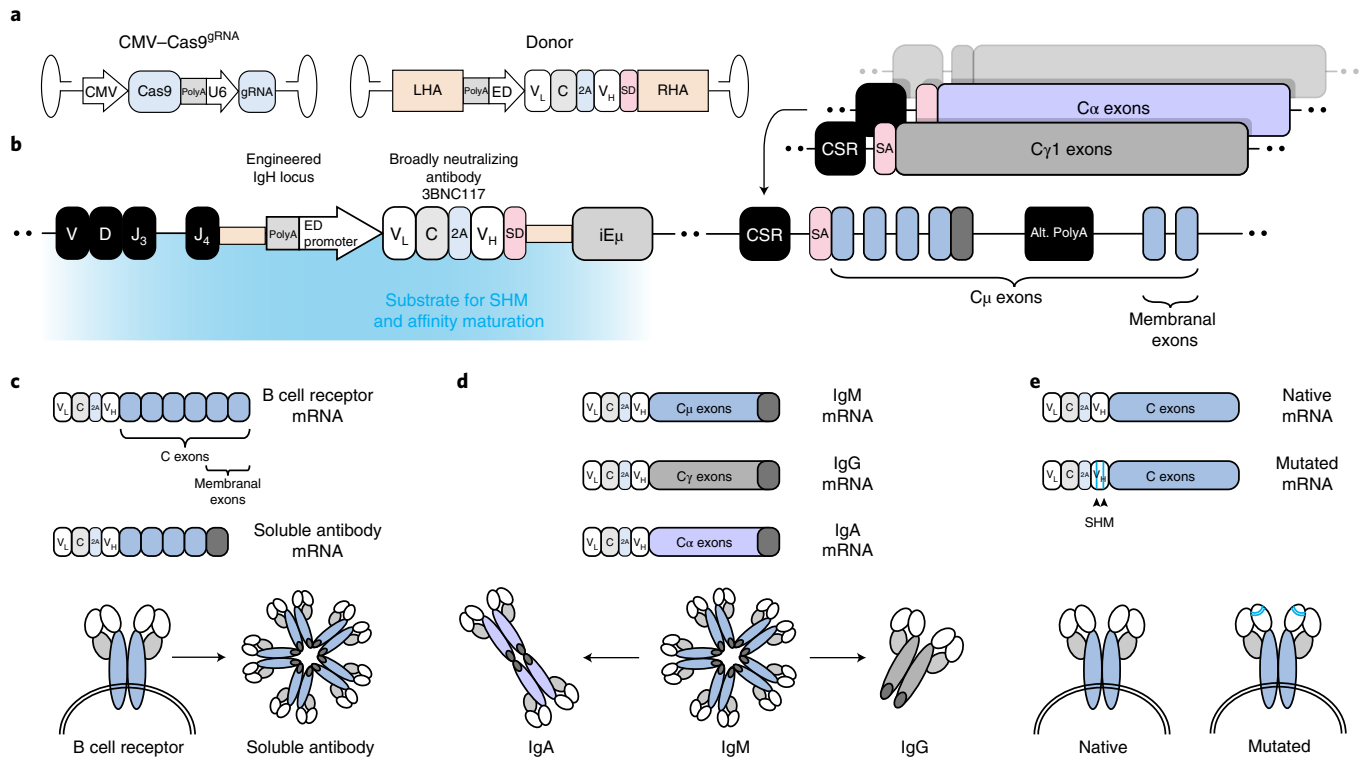

Fig. 1 | Targeting an antibody to the *IgH* locus of B cells to facilitate antigen-induced activation, SHM, CSR and affinity maturation. a, Design of the two AAV vectors. One vector codes for saCas9 and an sgRNA under CMV and U6 promoters, respectively. The second vector codes for the 3BNC117 bNAb cassette flanked by homology arms for integration into the CRISPR–Cas9 cut site at the J-C intron of the *IgH* locus. The bNAb cassette is expressed on integration under the control of an enhancer-dependent promoter (ED). The cassette includes the light chain in full and the variable segment of the heavy chain, separated by a sequence coding for a Furin cleavage site and a 2 A peptide. The variable heavy chain is followed by a splice donor sequence to allow fusion with the endogenous constant exons on integration, transcription and splicing. An upstream polyadenylation site is provided to terminate the transcription of the endogenous variable heavy chain on integration. **b**, Depiction of the *IgH* locus on integration. The bNAb cassette is integrated downstream of the last *J* segment (J_4) and upstream of the intronic enhancer (*iEμ*), CSR locus and the *IgHCμ* exons. **c**, The bNAb mRNA is terminated by alternative polyadenylation sites allowing for membranal (BCR) or soluble expression, before and after differentiation into a plasma cell, respectively. **d**, Different isotypes of the integrated antibody may be expressed on CSR of engineered B cells. **e**, SHM in the antibody coding genes may allow for affinity maturation and clonal expansion.

chain (V_H), separated by a sequence coding for a Furin cleavage site and for a 2A-peptide. A splice donor sequence follows the V_H gene segment to allow its fusion to constant *IgH* exons, on integration into the locus and subsequent transcription and splicing. Our design facilitates disruption of the endogenous *IgH* locus and initial bNAb expression as a membranal BCR. This allows for subsequent activation of the engineered B cells on antigen binding, which leads to differentiation into memory and plasma cells.

In vivo B cell engineering allows for high anti-HIV bNAb titers. AAV injections to mice were preceded by pre-immunizations, modeling a pre-existing infection. Indeed, B cell activation is required for efficient AAV transduction[30], and subsequent activation signals for the engineered B cells may benefit from previous priming of T helper cells and from presentation of appropriate immune complexes by follicular dendritic cells[31]. In particular, C57BL/6 mice were immunized with 20 μg of the gp120 HIV antigen, which is the target of 3BNC117. On day 6 postimmunization, each mouse was injected with 5×10^{11} viral genomes (vg) of a bNAb coding (donor) vector, 5×10^{11} vg of the saCas9 coding vectors or both (Fig. 2a). The mice then received additional immunizations on days 8, 23, 68, 98 and 128. Following the boosting regimen, mice receiving both a donor vector and an saCas9 vector had up to 5 μg ml^{-1} of the 3BNC117 bNAb in their blood, being >50× the median virus neutralization IC_{50} (half-maximum inhibitory concentration) for this bNAb[32,33] (Fig. 2b). This is in concordance with previous reports, entailing transfer of low numbers of antigen-specific B cells from transgenic mice, demonstrating a potent immune response following immunizations[34–36]. Here, 3BNC117 of multiple isotypes was found in the sera, and IgG 3BNC117 accounted for as much as 1% of the total response toward gp120 (Extended Data Fig. 1). IgG purified from treated mice can neutralize autologous YU2.DG and the heterologous tier-2 JRFL HIV pseudoviruses (Fig. 2c and Extended Data Fig. 2a). Mice injected with both a donor vector and an saCas9 vector had much higher 3BNC117 titers than mice receiving donor vector only. Nevertheless, 3BNC117 titers in mice receiving only the donor vector slightly exceeded the background levels measured in mice injected with PBS (Extended Data Fig. 2b). Indeed, integration of the antibody gene into the *IgH* locus was evident by PCR with with reverse transcription (RT–PCR) of splenic B cell RNA from mice receiving dual vector injection but an additional, nested PCR was required to detect such integration in two of the three mice injected with the donor vector alone (Extended Data Fig. 2c–e). Very low editing frequencies without CRISPR genomic RNA could similarly be detected by RT–PCR only in ex vivo edited lymphocytes (Extended Data Fig. 2f–i). Notably, when using dual vector injections, high titers could be obtained not only on immunizing the mice with the monomeric gp120 antigen of the clade B HIV strain YU2.DG, but also in independent experiments using either the clade A, BG505-based native trimer nanoparticle immu-

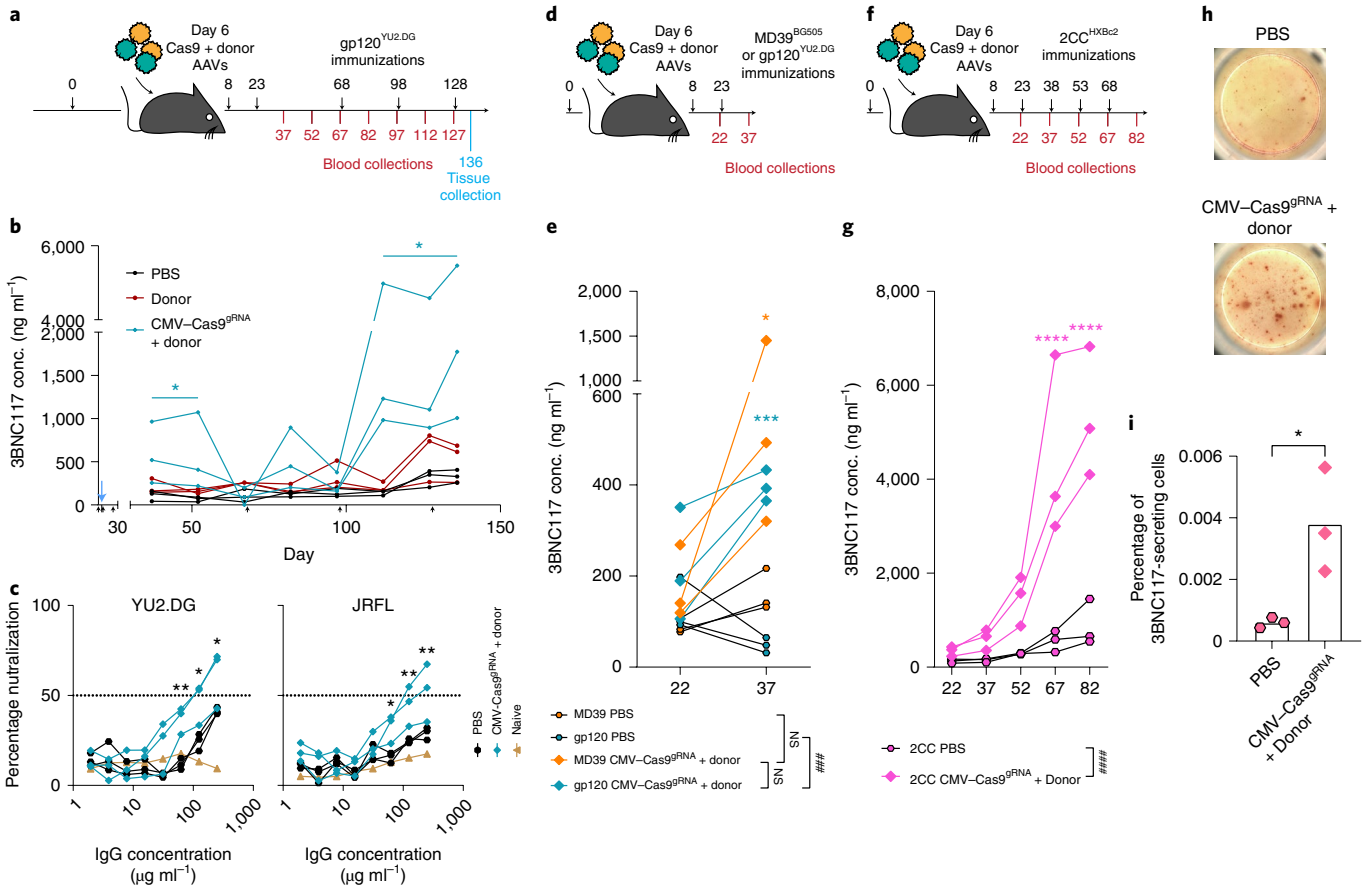

Fig. 2 | In vivo engineering of B cells to express an anti-HIV bNAb. a, Experimental scheme. Immunizations are indicated in black, above the timeline. Blood collections are indicated in red, below the timeline. **b**, 3BNC117 IgG titers as quantified by ELISA using an anti-idiotypic antibody to 3BNC117. The black arrows indicate immunizations and the blue arrow indicates the AAV injection. Each line represents a mouse. From left to right: $^{*}P = 0.047$, $P = 0.0201$ for two-way analysis of variance (ANOVA) of CMV-Cas9^{gRNA} + donor compared to the donor group. $n = 3$. AUC bar graphs are available in Extended Data Fig. 2. **c**, Transduction neutralization of TZM.bl cells by the YU2.DG (left) and JRFL (right) HIV pseudoviruses in the presence of IgGs purified from day 136 sera. Neutralization is calculated as percentage reduction from maximal luminescence per sample. The PBS control received immunizations as in **c**, while the naïve control represents serum IgG from an untreated mouse. Each line represents a mouse. From left to right: $^{*}P = 0.0306$, $P = 0.0116$, $^{**}P = 0.0037$, two-way ANOVA with Šidák's multiple comparison for time points comparison to PBS. AUC bar graphs are available in Extended Data Fig. 2. **d**,**e**, Experimental scheme (**d**) and 3BNC117 IgG titers (**e**) as quantified by ELISA for MD39 immunized mice. From left to right: not significant (NS), $P = 0.3724$ and $P = 0.0539$; $^{###}P = 0.0008$ for two-way ANOVA comparison between groups; and $^{*}P = 0.0493$, $^{***}P = 0.0007$ for two-way ANOVA with Šidák's multiple comparison for time points in comparison to antigen respective control. **f**,**g**, Experimental scheme (**f**) and 3BNC117 IgG titers (**g**) as quantified by ELISA for 2CC immunized mice. $^{####}P < 0.0001$ for two-way ANOVA comparison between groups and $^{****}P < 0.0001$ for two-way ANOVA with Šidák's multiple comparison for time points in comparison to PBS. **h**, A representative ELISPOT experiment of total bone marrows from 2CC immunized mice at day 82. **i**, Quantification of **h**. $^{*}P = 0.0317$ for two-sided unpaired *t*-test.

nogen (MD39-ferritin)[37] (Fig. 2d,e), or the stabilized soluble 2CC immunogen[38], originating from the clade B HXBc2 strain (Fig. 2f,g), attesting for the breadth of the 3BNC117-expressing cells in vivo. The presence of 3BNC117-secreting cells in the bone marrow was established using enzyme-linked immunosorbent spot (ELISPOT) on the bone marrow of treated mice (Fig. 2h,i) and correlated well with splenic 3BNC117 expression in these mice (Extended Data Fig. 3a,b).

In vivo engineered B cells undergo clonal expansion in germinal centers. The frequency of 3BNC117-expressing cells reached 0.5% of total blood B cells following the later immunizations in all mice injected with both a bNAb vector and an saCas9 vector, but not in mice injected with PBS or with the bNAb vector alone (Fig. 2a and Extended Data Fig. 3c,d). On euthanizing the mice at day 136, 8 days after the last immunization, up to 23% of the plasmablasts in the spleen (Fig. 3a,b and Extended Data Fig. 3e) and 5–10% of germinal center lymphocytes expressed 3BNC117 (Fig. 3c,d and Extended Data Fig. 3f).

Here, 0.6% of bone marrow cells expressed CD19 and 3BNC117 (Extended Data Fig. 3g,h). However, an additional 1.5% of bone marrow cells were CD19^{-}, 3BNC117^{+} (Extended Data Fig. 3g,i).

To study SHM and clonal selection, we extracted DNA from the liver and the spleen of one of the treated mice at day 136 and performed Illumina sequencing of amplified *3BNC117* V_H segments. Much of the mutation repertoire was shared between the liver and the spleen and may thus reflect heterogeneity in AAV production that is subjected to little or no selection[7,39]. In particular, all the *3BNC117* V_H variants found to be over-represented in the liver are also over-represented in the spleen. However, the inverse is not true. The complementarity-determining region-1 substitution R30K is the most prevalent substitution in the spleen. It accounts for more than 20% of all mutants in the spleen but is found at very low abundance in the liver or in a representative AAV batch

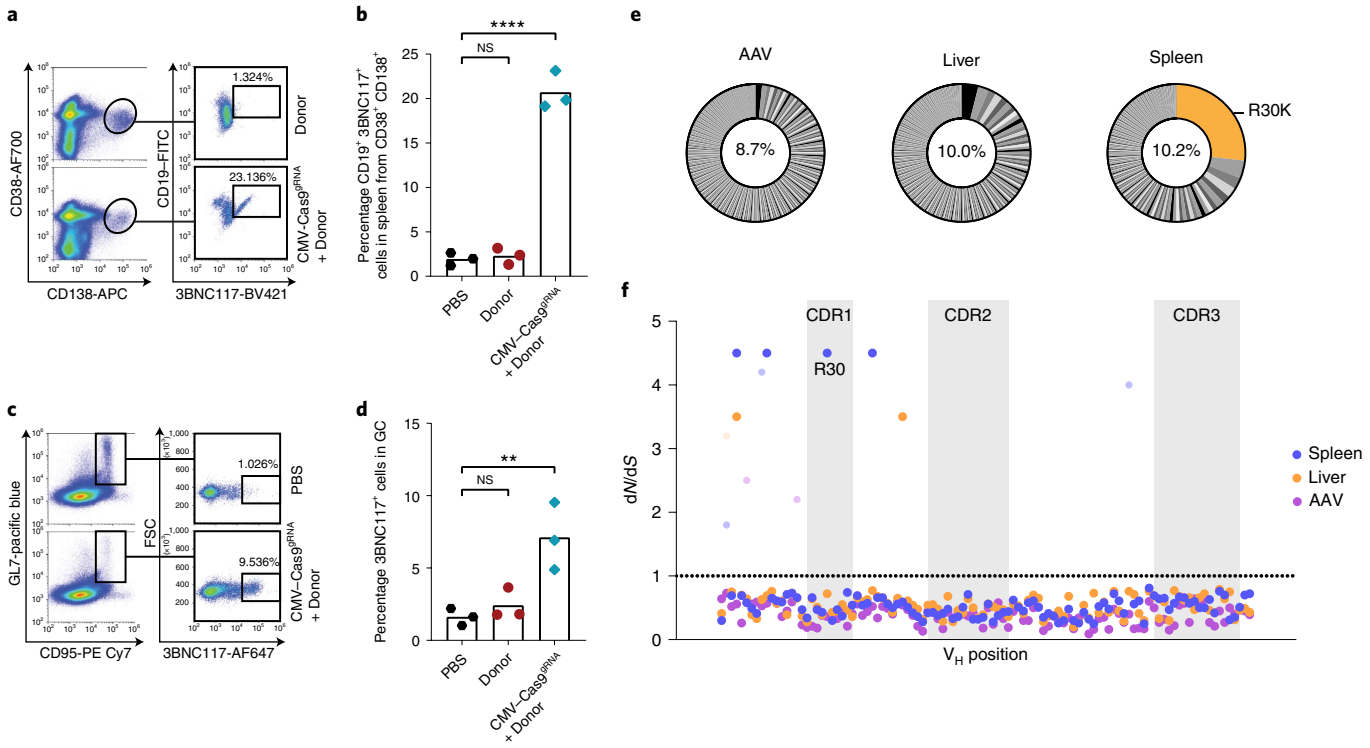

Fig. 3 | In vivo engineered B cells are found in lymphatic tissues 130 days following AAV injection. a, Flow cytometry plots demonstrating 3BNC117 expression among plasmablasts (CD38$^+$, CD138$^+$, CD19$^+$) in the spleen at day 136. Pregated on live, singlets. **b**, Quantification of **a** for engineered plasmablasts (CD38$^+$ CD138$^+$ 3BNC117$^+$). Mean is indicated by the bars. NS, $P = 0.9892$; ****$P < 0.0001$, one-way ANOVA with Tukey's multiple comparison. **c**, Flow cytometry plots demonstrating 3BNC117 expression of cells with a germinal center phenotype (GL7$^+$, CD95/Fas$^+$) in the spleen. Pregated on live, singlets. FSC, Fourier shell correlation. **d**, Quantification of **c**. Mean is indicated by the bars. GC, germinal center. NS, $P = 0.8916$; **$P = 0.0054$ one-way ANOVA with Tukey's multiple comparison. **e**, Pie charts of *3BNC117* V_H variants amplified from spleen and liver DNA at day 136 and from purified AAV. Orange shading indicates the R30K variant. Numbers in the middle of the pies indicate the total frequency of mutant reads in these samples. **f**, d*N*/d*S* values for the positions along the V_H segment, on the basis of Illumina sequencing of DNA amplified from the spleen (blue) or liver (orange) of a single mouse or AAV (purple). The dotted line represents values >1, indicative of positive selection. For dots colored with lighter shades, the assignment of a d*N*/d*S* value >1 is not statistically significant. No position in the AAV sample reached statistical significance. Gray shading indicates complementarity-determining region loops. The R30 position is indicated.

(Fig. 3e). Indeed, bNAbs of the VRC01 family were shown to have side-chain interactions with the HIV gp120 antigen at position 30 (ref. [29]). One may speculate that the conservative R30K substitution in 3BNC117 relieves some steric clash on binding to monomeric gp120. Including R30K, a total of four different positions along the V_H segment showed signs of positive selection in the spleen by analysis of the ratio of non-synonymous to synonymous mutations (d*N*/d*S*) and, as expected, none of which was enriched in the sequencing of the the representative AAV batch (Fig. 3f). We conclude that our in vivo engineering and immunization scheme has led to clonal expansion of variants stemming from either heterogeneity in AAV production or in vivo SHM. The clonal expansion is limited in span but pronounced in magnitude.

CRISPR–Cas9 cleavage is highly sequence specific but takes place also in undesired tissues. To assess the possible off-target effects of our in vivo engineering approach, we first quantified the copy number of the bNAb cassette in various tissues. The bNAb cassette was found at a high copy number in the liver at day 37 (Fig. 4a) and the levels were reduced by only tenfold at day 136 (Fig. 4b), reflecting high retention of AAV episomes in the liver. High copy number was also found in the blood at day 37, but levels dropped sharply by day 136, perhaps due to multiple cell divisions. The AAV copy number in the bone marrow was significantly increased from day 37 to day 136 and a nonsignificant similar trend was also detected in the lymph nodes, indicating the possible accumulation of 3BNC117-expressing cells in these tissues (Fig. 4b). The copy number in the liver was similar whether or not the saCas9 coding AAV was coinjected to the mice. In contrast, the copy number of the bNAb cassette in the lymph nodes and in the bone marrow was found to be logs higher with saCas9 AAV coinjection, signifying the selection of 3BNC117-expressing B cells (Fig. 4c).

To define the genome-wide off-target activity of saCas9, we performed circularization for high-throughput analysis of nuclease genome-wide effects by sequencing (CHANGE-seq)[40] on genomic DNA from C57BL/6 mice. Of the reads, 95% corresponded to the on-target site (Fig. 4d). We then performed targeted sequencing on four potential off-target sites, as well as on the on-target site, using gDNA from liver and spleen of treated mice and of a negative control mouse. Relative to control DNA from the spleen of an untreated mouse, a trend for a higher mutation rate, indicating error-prone repair of CRISPR–Cas9-induced double-stranded DNA breaks, was evident in the liver and not in the spleen, and only at the *IgH* on-target site rather than in any of the tested off-target sites (Fig. 4e).

To better characterize the different populations of engineered cells, we next used a donor vector coding for green fluorescent protein (GFP) in addition to the 3BNC117 cassette (Fig. 5a). Recipient mice were immunized twice before analysis of GFP and/or 3BNC117 expression in the bone marrow and the spleen (Fig. 5b). As expected, GFP$^+$, 3BNC117$^+$ cells were enriched in the spleen

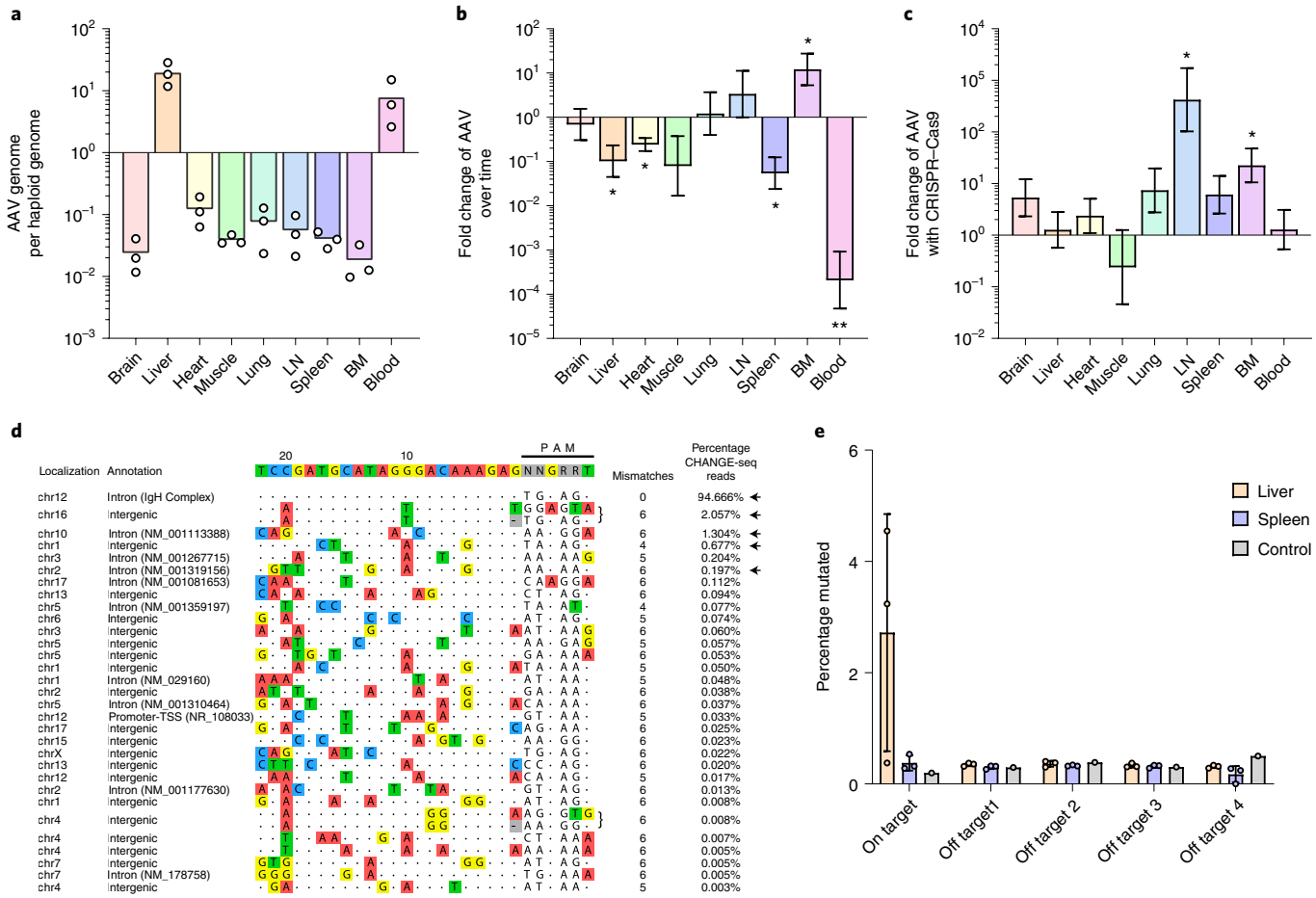

Fig. 4 | AAV biodistribution and saCas9 off-target cleavage analysis reveal a high safety profile. a, Donor AAV copy number quantification by qPCR in indicated tissues at day 136 from mice injected with two AAVs as in Fig. 2a. **b**, Relative copy number of donor AAV between days 37 and 136 in selected tissues. **c**, Relative copy number of donor AAV between mice injected with two AAVs, as in Fig. 2a, and mice injected with donor AAV only, at day 136. For **b** and **c**, indicated are the mean of relative expression and error bars corresponding to lower and upper boundaries derived from two-sided unpaired *t*-test. For **b**, from left to right: $^{*}P=0.0496$, $P=0.0139$, $P=0.0389$, $P=0.0243$; $^{**}P=0.0046$; comparison between the two time points. For **c**, from left to right: $^{*}P=0.0128$, $P=0.0147$ for comparison between the two mice groups. $n=3$ biologically independent animals. The *y* axes in **a**–**c** use a log scale. LN, lymph nodes and BM, bone marrow. **d**, Unbiased CHANGE-seq analysis of potential saCas9 off-target cleavage with the sgRNA used in this study. Localization, annotation in the genome, number of mismatches and percentage read counts are indicated for each on- or off-target site. Sequence of the sgRNA with the protospacer adjacent motif (PAM) is indicated on the top. Black arrows indicate target sites used for analysis of mouse samples. Mismatches between off-target sites and intended sgRNA target are color-coded. **e**, On- and off-target saCas9 cleavage, of target sites indicated in **d** by black arrows, in the spleen (mauve) and liver (beige) of mice injected with two AAVs, as in Fig. 2a, at day 136, as compared to uncut, naïve splenic lymphocytes DNA. For spleen and liver tissues, $n=3$ biologically independent animals. For the control uncut, naïve splenic lymphocyte DNA, $n=1$. Mean values ± s.d. are indicated.

(Fig. 5c and Extended Data Fig. 4a) and the bone marrow (Fig. 5d and Extended Data Fig. 4a) of mice receiving both the donor and the saCas9 vectors. Coinjection with donor and saCas9 vectors has increased the rate of B cells expressing GFP (Fig. 5e and Extended Data Fig. 4a) and, in particular, the rates of B cells expressing both GFP and 3BNC117 (Fig. 5c and Extended Data Fig. 4a) in the spleen. We estimate that, for a typical spleen of 50 M cells, assuming an expansion factor of 25-fold for antigen-specific B cells following a single immunization[34], as low as 140 cells may have been initially engineered. The rates of GFP$^+$, 3BNC117$^+$ cells among B220$^-$ cells remained low (Fig. 5c and Extended Data Fig. 4a). Notably, within the GFP expressing B cells, coinjecting the saCas9 vector led to a marked increase in 3BNC117$^+$, CD138$^+$ plasmablasts, in both the spleen (Fig. 5f and Extended Data Fig. 4a) and the bone marrow (Fig. 5g and Extended Data Fig. 4a). In the bone marrow, we found a larger fraction of cells, stained by the anti-3BNC117 anti-idiotype antibody, to be B220$^-$ (Extended Data Fig. 4a,b). The B220$^-$ cells, stained by the anti-idiotype, were almost exclusively CD3$^-$ and most of them were CD11b$^+$ cells (Extended Data Fig. 4a,c), indicative of possible FcR binding of secreted 3BNC117. Indeed, most of the CD11b$^+$ cells in the bone marrow, stained with the anti-idiotype, were GFP$^-$ (Extended Data Fig. 4d,e). In addition, the same anti-idiotype staining detected the ex vivo binding of soluble 3BNC117 by nonengineered CD11b$^+$ cells at a much higher rate than by nonengineered B220$^+$ cells (Extended Data Fig. 4f–i). An increase in the rate of cells, stained by the anti-idiotype, among GFP expressing cells was seen even within this B220$^-$ cell population in the spleen (Extended Data Fig. 4a,j) and marrow (Extended Data Fig. 4a,k). This is in line with recent publications showing expression of membrane antibodies by cells of the myeloid lineage[41–43]. Concordantly, we were able to ex vivo engineer CD11b$^+$ cells to express 3BNC117 from the *IgH* locus (Extended Data Fig. 4l–p). Cumulatively, our data indicate that, pending CRISPR–Cas9 mediated on-target integration, both B and non-B cells can express the antibody on the membrane, but only B cells proliferate subsequent to antigen engagement.

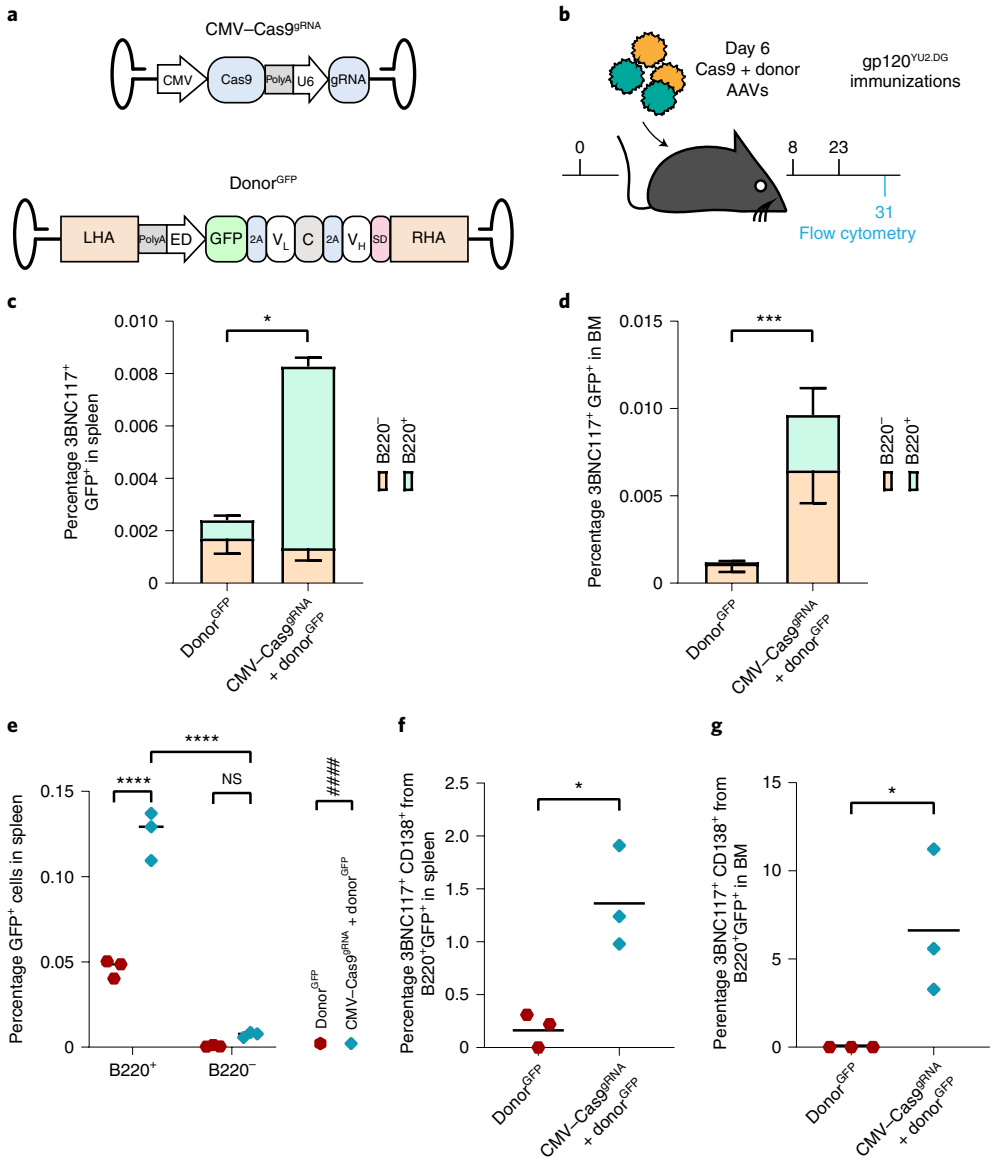

Fig. 5 | Assessing expression of the transgene in different subsets of cells. a, Vector design. The donor cassette expresses a GFP, separated from the 3BNC117 cassette by a 2A peptide. **b**, Experimental design. **c**,**d**, Quantification of GFP+ 3BNC117+ in the spleen (**c**) or bone marrow (**d**) of recipient mice. Mean values and standard deviation are indicated. For each group, $n=3$ biologically independent mice. *$P=0.0284$, ***$P=0.0004$ for two-way ANOVA. **e**, Quantification of GFP+ cells in spleen. ####$P<0.0001$ for two-way ANOVA and ****$P<0.0001$ for two-way ANOVA with Tukey's multiple comparison. **f**,**g**, Quantification of the 3BNC117+ CD138+ population from B220+, GFP+ cells in the spleen (**f**) *$P=0.0147$ for unpaired two-tailed *t*-test, or bone marrow (**g**) *$P=0.0471$ for unpaired two-tailed *t*-test. Mean values are indicated.

Coding the sgRNA and Cas9 on different vectors prevents cleavage in the absence of donor DNA. The coding of the single guide RNA (sgRNA) together with the saCas9 on the same AAV is predicted to allow DNA cleavage in many cells that are not cotransduced with the donor AAV. The resulting, nonproductive, cleavage may be avoided if the sgRNA cassette is instead separated from the saCas9 gene and coded on the donor AAV (Extended Data Fig. 5a). Repeating the above mouse experiments (Fig. 2a) with this new pair of AAVs allowed high 3BNC117 titers capable of neutralizing autologous YU2.DG and heterologous JRFL HIV pseudoviruses following repeated immunizations (Extended Data Fig. 5b–d), and the frequency of 3BNC117-expressing cells reached 0.5% of total blood B cells (Extended Data Fig. 5e,f). On killing the mice at day 136, up to 10% of splenic plasmablasts expressed 3BNC117 (Extended Data Fig. 5g,h). In addition, up to 7% of splenic B cells with a germinal center phenotype expressed 3BNC117 (Extended Data Fig. 5i,j), while 1 and 3% of the bone marrow cells expressed 3BNC117, with or without coexpressing CD19, respectively (Extended Data Fig. 5k–m). These results are of the same range as those obtained when the sgRNA was coded together with the saCas9, although direct side-by-side comparison is hindered by the use of different ubiquitously active promoters. The overall numbers of splenic plasmablasts, germinal center B cells and bone marrow plasma cells were similar to those in the control groups (Extended Data Fig. 5n,o), mitigating concerns of B cell neoplasm (Extended Data Fig. 3e,f).

Driving Cas9 expression by a B cell-specific promoter prevents cleavage in undesired tissues. To further increase the safety of our approach, we next coded the saCas9 under the control of the CD19, B cell-specific, promoter[44] (Fig. 6a). In particular, C57BL/6 mice

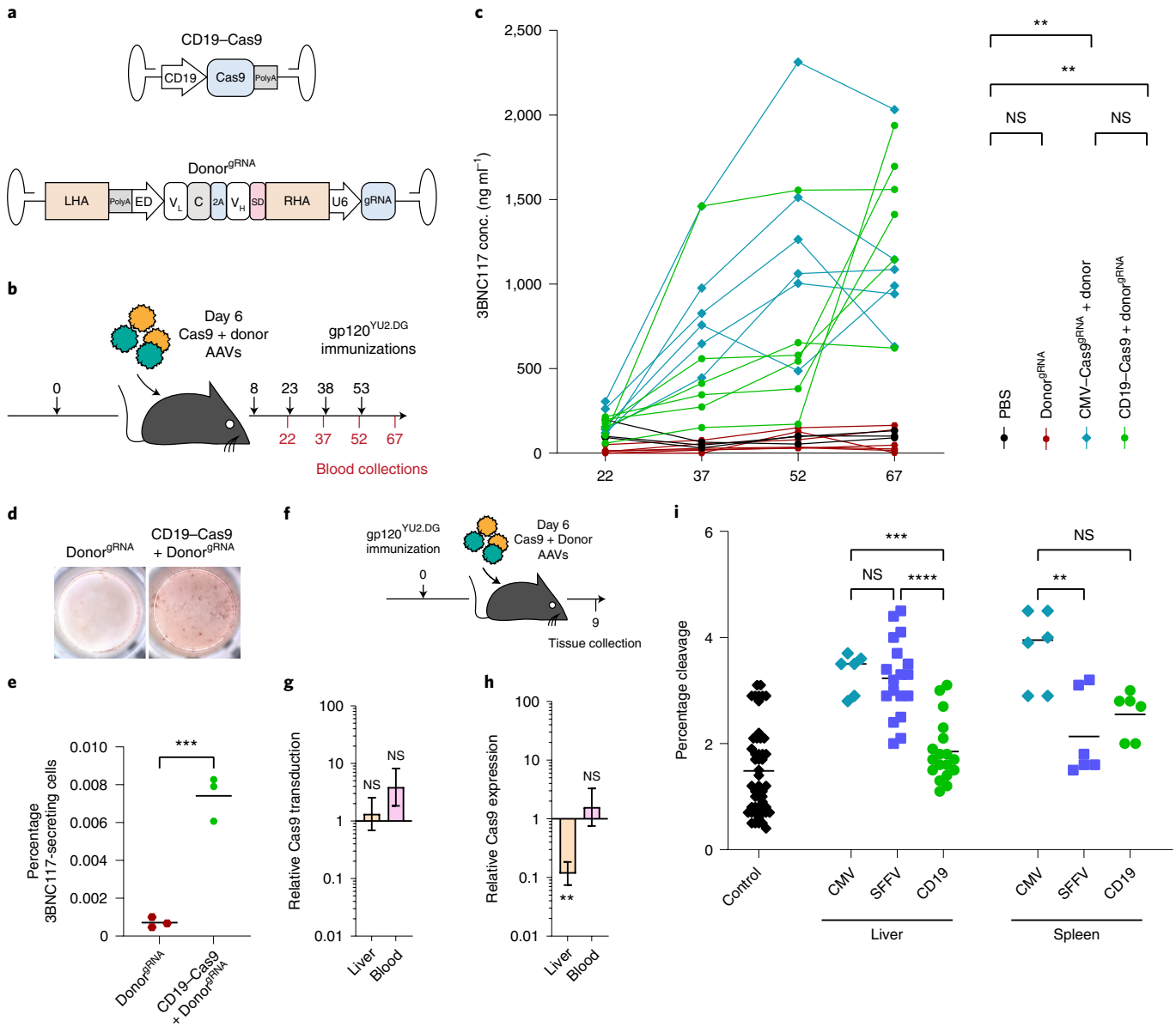

Fig. 6 | Improving safety by coding saCas9 and the sgRNA on separate AAVs and expressing saCas9 under the regulation of a B cell-specific promoter. **a**, Map of the AAV vectors used. saCas9 is expressed under the CD19 promoter, while the sgRNA is coded on the donor vector, outside the homology arms. **b**, Experimental scheme. Mice were immunized according to the timeline in black (top), and bled as indicated in red (bottom). **c**, 3BNC117 IgG titers, quantified by ELISA with an anti-idiotypic antibody. Each line represents a mouse. From top to bottom and left to right: $^{**}P = 0.0075$, and $P = 0.0055$, NS; $P = 0.0876$ and $P = 0.3288$ for two-way ANOVA. **d**, Representative ELISPOTs of bone marrows from mice, 45 days following the fourth immunization. **e**, Quantification of **d**. $^{***}P = 0.0007$ for two-sided unpaired *t*-test. **f**, Experimental scheme. Mice immunized with gp120 are dosed with AAVs and tissues are collected 3 days following AAV injection. **g**, Relative transduction by the saCas9 coding AAV, calculated as the ratio of copy numbers, in the indicated tissues, between mice receiving AAVs coding for saCas9 under the CD19 or SFFV promoters. Indicated are the mean of relative expression and error bars corresponding to lower and upper boundaries derived from two-sided unpaired *t*-test. From left to right: NS; $P = 0.6920$ and $P = 0.1441$. $n = 3$ biologically independent animals. **h**, Relative *saCas9* mRNA expression, depicted as the ratio between *saCas9* expression from the CD19 promoter and from the SFFV promoter. Indicated are the mean of relative expression and error bars corresponding to lower and upper boundaries derived from two-sided unpaired *t*-test. NS; $P = 0.5698$, $^{**}P = 0.0092$. $n = 3$ biologically independent animals. **i**, TIDE analysis of on-target cleavage in the indicated tissues using CMV, SFFV or CD19 driven saCas9 expression. From left to right: NS; $P > 0.9999$ and $P = 0.0760$, $^{**}P = 0.0036$, $^{***}P = 0.0008$, $^{****}P < 0.0001$ for one-way ANOVA with Tukey's multiple comparison. Each dot represents a comparison between a control sequence and an independent mouse sequence.

were immunized with 20 µg of HIV gp120, and 6 days later each mouse was coinjected with one vector coding for saCas9, regulated by the CD19 promoter, and a second vector coding both the bNAb and the sgRNA (Fig. 6a,b). The mice then received up to six additional immunizations. Already, after four immunizations, treated mice had up to 2 µg ml^{-1} of the 3BNC117 bNAb in their blood (Fig. 6c). 3BNC117 blood titers did not go down by 30 days later, irrespective of whether additional immunizations were administered (Extended Data Fig. 6a). Regardless of the immunization regimen, similar titers were obtained using promiscuous or B cell-specific regulation over saCas9 expression. Concordantly, 45 days after the fourth immunization, similar rates of 3BNC117-secreting cells

could be detected in the bone marrow using ELISPOT (Fig. 6d,e), irrespective of whether additional immunizations were administered and irrespective of the saCas9 promoter (Extended Data Fig. 6b–d). Therefore, replacing the saCas9 promoter does not preclude the therapeutic effect, which is stable after four immunizations. In addition, using CD19 rather than CMV promoter, to drive saCas9 expression, reduces the engineering rate of B cell progenitors as assessed following in vitro differentiation of IL7R enriched bone marrow cells (Extended Data Fig. 7). Even when the CMV promoter is used to drive saCas9 expression, bone marrow hematopoietic stem and progenitor cells may not be engineered, as similarly low 3BNC117 staining and enzyme-linked immunosorbent assay (ELISA) levels are obtained following syngeneic transplantation of Lin^- enriched cells from mice injected with the donor vector with or without the saCas9 coding vector (Extended Data Fig. 8).

To assess possible effects on biodistribution and safety, different groups of mice were euthanized for tissue analysis, 3 days after having been coinjected with the donor + sgRNA vector and with a second vector coding for saCas9 under the control of either a ubiquitous promoter or the B cell-specific CD19 promoter. Similar transduction rates were obtained for vectors coding the saCas9 under the regulation of the CD19 or spleen focus forming virus (SFFV) promoters (Fig. 6f,g). However, the CD19 promoter significantly reduced *saCas9* expression in the liver, while not reducing expression in peripheral blood mononuclear cells (Fig. 6h). The rates of on-target cleavage in the liver or the spleen, as measured by TIDE analysis, were significantly above background only when using the CMV or SFFV promoters, rather than the CD19 promoter, to drive saCas9 expression (Fig. 6i). Therefore, separating the coding of saCas9 and the sgRNA between the two AAVs and expressing saCas9 under a B cell-specific promoter reduce undesired cleavage to below our limit of detection while allowing high 3BNC117 titers following immunizations.

Discussion

Eliciting a specific, neutralizing antibody response to hypervariable viruses is a long-standing challenge in medicine. B cell engineering provides an opportunity to express desired therapeutic antibodies for adaptive immunity. Here, we uniquely demonstrate that B cells can be safely and robustly engineered in vivo. A single, systemic dose of dual AAV-DJ coding for CRISPR–Cas9 and donor cassettes in mice allowed for site-specific integration, with limited off-target Cas9 expression and DNA double-strand breaks. On immunizations, the engineered B cells underwent antigen-induced activation leading to memory retention, clonal selection and differentiation into plasma cells that secrete the bNAb at neutralizing levels.

The monoclonal bNAb titers obtained by in vivo engineering in this work are similar or higher than those obtained by ex vivo engineering followed by adoptive transfer to immunocompetent mice[7,12,13], with the exception of Huang et al[8]. The response of the in vivo engineered B cells to the antigen is not hindered by the endogenous polyclonal response to immunization, which can be highly potent[45]. In contrast to ex vivo engineering, in vivo B cell engineering is simple, fast and cost effective. It can and will be provided at the point of care, requiring no specialized facilities. Our approach further allows for CSR and clonal expansion, but the full functional consequences of these attributes will have to be tested in the prevention or treatment of infection models. Yet additional experiments may determine whether in vivo B cell engineering allows proper antibody glycosylation and expression patterns to avoid the formation of antidrug antibodies, as seen following muscle transduction for antibody expression[6]. The effects of anti-AAV antibodies and T cell responses would similarly have to be assessed. In engineered B cells, autoreactivity may occur due to heterogeneity in AAV production or due to pairing of the engineered heavy chain with the endogenous light chain. Future clinical applications must aim to reduce these sources of heterogeneity, if not sufficiently eliminated by natural tolerance mechanisms[46,47]. Still, future modifications may include coding the bNAb as a single chain[13] to reduce mispairing of the bNAb heavy chain with the endogenous light chain, potentially improving both safety and efficacy. Such single chain coding can further allow the expression of bispecific bNAbs, which may be required to provide long-term protection from HIV resurgence[1]. Safety may be further improved by using more specific nucleases[48,49] and by having the bNAb gene preceded by a splice acceptor rather than by a promoter, to reduce expression from off-target integration[7,12]. Both safety and efficacy may benefit from embedding B cell-specific targeting moieties in the AAV vector[50] or in a nonviral alternative[14]. The therapeutic impact of our approach may best be evaluated in nonhuman primates with HIV-like infections. In the nonhuman primates as in HIV infected individuals, undergoing controlled treatment interruption, we expect a continuous and much more potent antigen-induced activation, which can either replace or complement an immunization regimen to achieve higher antibody titers and do so in a shorter time frame. Finally, in vivo B cell engineering may have diverse future applications as it may be used to address other persistent infections as well as to treat autoimmune diseases, genetic disorders and cancer.

Online content

Any methods, additional references, Nature Research reporting summaries, source data, extended data, supplementary information, acknowledgements, peer review information; details of author contributions and competing interests; and statements of data and code availability are available at https://doi.org/10.1038/s41587-022-01328-9.

Received: 15 February 2021; Accepted: 22 April 2022;
Published online: 09 June 2022

References

1. Mendoza, P. et al. Combination therapy with anti-HIV-1 antibodies maintains viral suppression. *Nature* **561**, 479–484 (2018).
2. Bar-On, Y. et al. Safety and antiviral activity of combination HIV-1 broadly neutralizing antibodies in viremic individuals. *Nat. Med.* **24**, 1701–1707 (2018).
3. Cohen, Y. Z. et al. Safety, pharmacokinetics, and immunogenicity of the combination of the broadly neutralizing anti-HIV-1 antibodies 3BNC117 and 10-1074 in healthy adults: a randomized, phase 1 study. *PLoS ONE* **14**, e0219142 (2019).
4. Johnson, P. R. et al. Vector-mediated gene transfer engenders long-lived neutralizing activity and protection against SIV infection in monkeys. *Nat. Med.* **15**, 901–906 (2009).
5. Balazs, A. B. et al. Vectored immunoprophylaxis protects humanized mice from mucosal HIV transmission. *Nat. Med.* **20**, 296–300 (2014).
6. Priddy, F. H. et al. Adeno-associated virus vectored immunoprophylaxis to prevent HIV in healthy adults: a phase 1 randomised controlled trial. *Lancet HIV* **6**, e230–e239 (2019).
7. Nahmad, A. D. et al. Engineered B cells expressing an anti-HIV antibody enable memory retention, isotype switching and clonal expansion. *Nat. Commun.* **11**, 5851 (2020).
8. Huang, D. et al. Vaccine elicitation of HIV broadly neutralizing antibodies from engineered B cells. *Nat. Commun.* **11**, 5850 (2020).
9. Fusil, F. et al. A lentiviral vector allowing physiologically regulated membrane-anchored and secreted antibody expression depending on B-cell maturation status. *Mol. Ther.* **23**, 1734–1747 (2015).
10. Greiner, V. et al. CRISPR-mediated editing of the B cell receptor in primary human B cells. *Science* **12**, 369–378 (2019).
11. Voss, J. E. et al. Reprogramming the antigen specificity of B cells using genome-editing technologies. *eLife* **8**, e42995 (2019).
12. Hartweger, H. et al. HIV-specific humoral immune responses by CRISPR/Cas9-edited B cells. *J. Exp. Med.* **216**, 1301–1310 (2019).
13. Moffett, H. F. et al. B cells engineered to express pathogen-specific antibodies protect against infection. *Sci. Immunol.* **4**, eaax0644 (2019).
14. Smith, T. T. et al. In situ programming of leukaemia-specific t cells using synthetic DNA nanocarriers. *Nat. Nanotechnol.* **12**, 813–822 (2017).
15. Agarwal, S. et al. In vivo generation of CAR T cells selectively in human $CD4^+$ lymphocytes. *Mol. Ther.* **28**, 1783–1794 (2020).

16. Agarwal, S., Weidner, T., Thalheimer, F. B. & Buchholz, C. J. In vivo generated human CAR T cells eradicate tumor cells. *Oncoimmunology* **8**, e167161 (2019).
17. Frank, A. M. et al. Combining T-cell-specific activation and in vivo gene delivery through CD3-targeted lentiviral vectors. *Blood Adv.* **4**, 5702–5715 (2020).
18. Frank, A. M. & Buchholz, C. J. Surface-engineered lentiviral vectors for selective gene transfer into subtypes of lymphocytes. *Mol. Ther. Methods Clin. Dev.* **12**, 19–31 (2019).
19. Frank, A. M. et al. CD8-specific designed ankyrin repeat proteins improve selective gene delivery into human and primate T lymphocytes. *Hum. Gene Ther.* **31**, 679–691 (2020).
20. Pfeiffer, A. et al. In vivo generation of human CD19-CAR T cells results in B-cell depletion and signs of cytokine release syndrome. *EMBO Mol. Med.* **10**, e9158 (2018).
21. Michels, A. et al. Lentiviral and adeno-associated vectors efficiently transduce mouse T lymphocytes when targeted to murine CD8. *Mol. Ther. Methods Clin. Dev.* **23**, 334–347 (2021).
22. Münch, R. C. et al. Off-target-free gene delivery by affinity-purified receptor-targeted viral vectors. *Nat. Commun.* **6**, 2–10 (2015).
23. Breuer, C. B. et al. In vivo engineering of lymphocytes after systemic exosome-associated AAV delivery. *Sci. Rep.* **10**, 4544 (2020).
24. Nawaz, W. et al. AAV-mediated in vivo CAR gene therapy for targeting human T-cell leukemia. *Blood Cancer J.* **11**, 119 (2021).
25. Rurik, J. G. et al. CAR T cells produced in vivo to treat cardiac injury. *Science* **375**, 91–96 (2022).
26. Parayath, N. N., Stephan, S. B., Koehne, A. L., Nelson, P. S. & Stephan, M. T. In vitro-transcribed antigen receptor mRNA nanocarriers for transient expression in circulating T cells in vivo. *Nat. Commun.* **11**, 6080 (2020).
27. Grimm, D. et al. In vitro and in vivo gene therapy vector evolution via multispecies interbreeding and retargeting of adeno-associated viruses. *J. Virol.* **82**, 5887–5911 (2008).
28. Ran, F. A. et al. In vivo genome editing using *Staphylococcus aureus* Cas9. *Nature* **520**, 186–191 (2015).
29. Scheid, J. F. et al. Sequence and structural convergence of broad and potent HIV antibodies that mimic CD4 binding. *Science* **333**, 1633–1637 (2011).
30. Hung, K. L. et al. Engineering protein-secreting plasma cells by homology-directed repair in primary human B cells. *Mol. Ther.* **26**, 456–467 (2018).
31. Mesin, L., Ersching, J. & Victora, G. D. Germinal center B cell dynamics. *Immunity* **45**, 471–482 (2016).
32. Sok, D. & Burton, D. R. HIV broadly neutralizing antibodies: taking good care of the 98%. *Immunity* **45**, 958–960 (2016).
33. Garber, D. A. et al. Durable protection against repeated penile exposures to simian-human immunodeficiency virus by broadly neutralizing antibodies. *Nat. Commun.* **11**, 3195 (2020).
34. Taylor, J. J., Pape, K. A., Steach, H. R. & Jenkins, M. K. Apoptosis and antigen affinity limit effector cell differentiation of a single naïve B cell. *Science* **347**, 11214–11218 (2015).
35. Abbott, R. K. et al. Precursor frequency and affinity determine B cell competitive fitness in germinal centers, tested with germline-targeting HIV vaccine immunogens. *Immunity* **48**, 133–145.e6 (2017).
36. Dosenovic, P. et al. Anti-HIV-1 B cell responses are dependent on B cell precursor frequency and antigen binding affinity. *Proc. Natl Acad. Sci. USA* **115**, 4743–4748 (2018).
37. Dey, B. et al. Structure-based stabilization of HIV-1 gp120 enhances humoral immune responses to the induced co-receptor binding site. *PLoS Pathog.* **5**, e1000445 (2009).
38. Steichen, J. M. et al. HIV vaccine design to target germline precursors of glycan-dependent broadly neutralizing antibodies. *Immunity* **45**, 483–496 (2016).
39. Lecomte, E. et al. Advanced characterization of DNA molecules in rAAV vector preparations by single-stranded virus next-generation sequencing. *Mol. Ther. Nucleic Acids* **4**, e260 (2015).
40. Lazzarotto, C. R. et al. CHANGE-seq reveals genetic and epigenetic effects on CRISPR–Cas9 genome-wide activity. *Nat. Biotechnol.* **38**, 1317–1327 (2020).
41. Busch, S. et al. Circulating monocytes and tumor-associated macrophages express recombined immunoglobulins in glioblastoma patients. *Clin. Transl. Med.* **8**, 18 (2019).
42. Gong, X. et al. Macrophage-derived immunoglobulin M inhibits inflammatory responses via modulating endoplasmic reticulum stress. *Cells* **10**, 2812 (2021).
43. Fuchs, T. et al. Expression of combinatorial immunoglobulins in macrophages in the tumor microenvironment. *PLoS ONE* **13**, e0204108 (2018).
44. Moreau, T., Bardin, F., Imbert, J., Chabannon, C. & Tonnelle, C. Restriction of transgene expression to the B-lymphoid progeny of human lentivirally transduced CD34$^+$ cells. *Mol. Ther.* **10**, 45–56 (2004).
45. McCarron, M. J., Park, P. W. & Fooksman, D. R. CD138 mediates selection of mature plasma cells by regulating their survival. *Blood* **129**, 2749–2759 (2017).
46. Nemazee, D. Mechanisms of central tolerance for B cells. *Nat. Rev. Immunol.* **17**, 281–294 (2017).
47. Russell, D. M. et al. Peripheral deletion of self-reactive B cells. *Nature* **354**, 308–311 (1991).
48. Edraki, A., Mir, A., Ibraheim, R., Gainetdinov, I. & Sontheimer, E. J. A compact, high-accuracy Cas9 with a dinucleotide PAM for in vivo genome editing. *Mol. Cell* **73**, 714–726 (2019).
49. Pausch, P. et al. CRISPR-CasΦ from huge phages is a hypercompact genome editor. *Science* **337**, 333–337 (2020).
50. Hartmann, J. et al. A library-based screening strategy for the identification of DARPins as ligands for receptor-targeted AAV and lentiviral vectors. *Mol. Ther. Methods Clin. Dev.* **10**, 128–143 (2018).

Methods

Plasmid cloning. For the CMV–Cas9^{gRNA} vector, pX601 (ref. [28]) (Addgene) was cleaved with BsaI and pre-annealed, phosphorylated (PNK, NEB), sgRNA coding oligo-deoxynucleotides were ligated using T4 DNA Ligase (NEB). For the CD19–Cas9 vector, pAB270 (ref. [51]) was cleaved using NotI and SpeI (NEB) and an saCas9 coding fragment, amplified from pX601, as well as the murine CD19 promoter, amplified from wild type C57BL/6OlaHsd gDNA, were assembled using Hi-Fi DNA Assembly Mix (NEB). For the SFFV–Cas9 vector, pAB270 was cleaved with NotI and SpeI (NEB). The fragment coding the SFFV promoter was amplified from GW175 (Kay Laboratory, Stanford) and the saCas9 was amplified from pX601. The fragments were assembled using Hi-Fi DNA Assembly Mix (NEB). For the donor^{gRNA} vector, the U6-gRNA fragment was amplified from ligated pX601 with the murine *IgH* sgRNA used in this study, and the fragment was assembled using Hi-Fi DNA Assembly Mix (NEB) into the donor vector pADN171XS (ref. [7]), following cleavage with SpeI (NEB). For cloning of the GFP-3BNC117-expressing donor (Fig. 3a), Hi-Fi DNA Assembly (NEB) was performed according to the manufacturer's instructions using a fragment amplified from pADN171XS (donor vector from Nahmad et al.[7] and named 'donor' in this paper), a fragment amplified from pADN157CF2 (GFP expressing vector from Nahmad et al.[7]) and a homology arms-bearing vector cleaved with XhoI[7]. A list of primers used for these reactions can be found in Supplementary Table 1. The resulting plasmid was Sanger sequenced for verification of the correct integration of the fragments into the vector.

A list of primers used for cloning can be found in Supplementary Table 1. All fragments for cloning were amplified using PrimeStar MAX (Takara).

rAAV production. rAAV-DJ were produced in human embryonic kidney 293T (HEK293T) cells (ATCC) by triple transient transfection using polyethylenimine (Polysciences Inc). For each vector, 14 15-cm dishes were transfected at 80% confluency with pAd5 (helper plasmid), rAAV-DJ genome plasmid and vector plasmid at a 3:1:1 ratio[27]. In total, each plate was transfected with 41.25 µg of DNA. Purification was performed with AAVpro Extraction Kit (Takara) according to the manufacturer's protocol. Titer quantification was performed by quantitative PCR (qPCR) using SYBRGreen (PCR Biosystems). A list of primers used for AAV titer quantification can be found in Supplementary Table 1.

Mouse studies. Mouse experiments comply with all ethical regulations and were performed under supervision of Tel Aviv University Committee for the Use and Treatment of Laboratory Animals. In vivo engineering experiments were performed on 6–10 weeks old female CD45.2 C57BL/6OlaHsd (Envigo) mice. All mice were housed and kept at ambient temperature of 19–23 °C, humidity of 45–65% and with a 12-h light/12-h dark cycle. Immunizations with gp120-YU2 or MD39-ferritin were performed as previously described, using 20 µg per mouse of antigen in Alum (Invitrogen)[7,8]. For AAV injections, mice were anesthetized with 0.1 and 0.001 mg g^{-1} Ketamine and Xylazine, respectively, and were injected i.v. with 5×10^{11} vg per vector per 100 µl per mouse in PBS. Blood samples from mice were collected in heparin. Cells and serum were separated by centrifugation. Serum was collected from the supernatant. For spleens, whole spleens were extracted from mice and mechanically crushed in PBS to be filtered in a 70-µm cell strainer (Corning). For bone marrow, cells were flushed from the posterior femur and tibia. For blood, spleen and bone marrow, cells were processed with red blood cell (RBC) lysis buffer (Biolegend) and plated in 1640 RPMI (Biological Industries) supplemented with 10% HI fetal bovine serum (FBS) (Biological Industries) until processing. Muscle tissue was processed from femoral muscles. Right or left lungs were processed for pulmonic tissue. Right or left hemispheres were processed for brain tissue. Lobes were processed for liver tissue and whole heart was used for cardiac tissue. For lymph nodes, inguinal and cervical lymph nodes were pooled for processing.

Illumina sequencing and analysis. Total gDNA was extracted from fresh tissues using Gentra PureGene Tissue Kit (Qiagen). Initial PCR amplification and the subsequent barcoding PCR reaction of the *3BNC117* V_H fragments or the off-target sites was performed using the proofreading PrimeStarMAX Polymerase (Takara) for 35 cycles and eight cycles, respectively. A list of primers used for these reactions can be found in Supplementary Table 1. Following each PCR, amplicons were purified using AMPure XP beads (Beckman Coulter) at a 0.7:1 ratio. Libraries were quantified using Qubit (Invitrogen) and analyzed using an Agilent 4200 TapeStation. Combined libraries were loaded at 5 pM with 25% PhiX control (Illumina) and sequencing was performed with a v.2 Nano Reagent kit 2×250 bp on a MiSeq machine, using the MiSeq control software, at the Genomic Research Unit, Tel Aviv University. For off-target analysis, raw fastq files were submitted to fast length adjustment of short reads (FLASH) (https://github.com/ebiggers/flash)[52]. The default parameters were changed to allow for lower maximum mismatch density ratio of 0.1. The resultant files were submitted to CRISPRpic (https://github.com/compbio/CRISPRpic)[53], with a wider mutagenic window of 10 bp on either side of the DNA double-strand breaks. Presented data pools all mutation types detected.

For mutation and selection analysis, raw fastq files were submitted to FLASH using the default parameters. The resultant files submitted to Bowtie2 alignment analysis (https://github.com/BenLangmead/bowtie2)[54] compared to the engineered *3BNC117* sequence, using local mode and the 'xeq' parameter for match and mismatch annotations. Using a specific script, unaligned reads were filtered, as well as reads not within 80–115% of the original length and reads with more than 15% mutated bases. The primer annealing sites at both ends of the sequences were omitted from the analysis. All bases considered as mutated in this analysis had a *Q* score higher than 20. The Selecton software[55] was used to run M8 and M8a models to infer positive selection and likelihood ratio test was performed between the null model (M8a) and the alternative model (M8) to determine which model better fits the data. All *P* values were corrected for multiple testing using false discovery rate (FDR)[56]. For d*N*/d*S* and clonal expansion analyses, to reduce sequencing biases, an additional three nucleotides on both ends of the sequencing were removed. All alignments and phylogenies supported the M8 alternative model where positive selection is enabled.

CHANGE-seq. gDNA from fresh spleens of wild type C57BL/6OlaHsd using Gentra PureGene Tissue Kit (Qiagen) and quantified using Qubit (Invitrogen) according to the manufacturer's instructions. CHANGE-seq was performed as previously described[40]. Briefly, purified genomic DNA was tagmented with a custom Tn5-transposome to an average length of 400 bp, followed by gap repair with Kapa Hi-Fi HotStart Uracil+ DNA Polymerase (KAPA Biosystems) and Taq DNA Ligase (NEB). Gap-repaired tagmented DNA was treated with USER enzyme (NEB) and T4 polynucleotide kinase (NEB). Intramolecular circularization of the DNA was performed with T4 DNA Ligase (NEB) and residual linear DNA was degraded by a cocktail of exonucleases containing Plasmid-Safe ATP-dependent DNase (Lucigen), Lambda exonuclease (NEB) and Exonuclease I (NEB). In vitro cleavage reactions were performed with 125 ng of exonuclease-treated circularized DNA, 90 nM of EnGen Sau Cas9 protein (NEB), NEB buffer 3.1 (NEB) and 270 nM of sgRNA (Synthego), in a 50 µl volume. Cleaved products were A-tailed, ligated with a hairpin adaptor (NEB), treated with USER enzyme (NEB) and amplified by PCR with barcoded universal primers NEBNext Multiplex Oligos for Illumina (NEB), using Kapa Hi-Fi Polymerase (KAPA Biosystems). Libraries were quantified by qPCR (KAPA Biosystems) and sequenced with 151 bp paired-end reads on an Illumina MiniSeq instrument. CHANGE-seq data analyses were performed using open-source CHANGE-seq analysis software (https://github.com/tsailabSJ/changeseq).

ELISA. High binding microplates (Greiner Bio-One) were coated with 2 µg ml^{-1} of an anti-idiotipic antibody against 3BNC117 in PBS overnight at 4 °C. Plates were washed with PBS with Tween (PBST), blocked for 1 h with 5% BSA in PBST and washed again. For 3BNC117 IgG quantification, samples were diluted 1:50–500-fold and a standard was made using purified 3BNC117 serially diluted in PBS. For 3BNC117 isotype detection, samples were serially diluted as described in the figures. Samples and standards were incubated for 1 h. Plates were then applied with horseradish peroxidase-conjugated detection antibodies: antimouse IgA (Abcam), antimouse IgG, antimouse IgG1, antimouse IgM (Jackson ImmunoResearch) or antimouse IgG2c (Bio-Rad Laboratories) at 2 µg ml^{-1} in PBST and were incubated for another hour. A list of antibodies used in these experiments may be found in Supplementary Table 1. Before detection with QuantaBlu (ThermoFisher) according to the manufacturer's protocol, plates were washed for an additional round. Detection was done in a Synergy M1 Plate reader (Biotek). When absolute quantitation is presented, the concentration of 3BNC117 was determined by reference to the dilution factor of the standard curve.

To quantify the fraction of 3BNC117 from the gp120 response, we performed Dynabead purification of sera. In short, for each sample, 5 mg of Dynabeads M-280 Tosylactivated (Invitrogen) were conjugated with 50 µg of gp120 in 0.1 M Na-Phosphate supplemented at a 1.5:1 ratio of 3 M ammonium sulfate buffer at 37 °C overnight. Beads were then washed, blocked with 0.5% BSA in PBS for 1 h at 37 °C, washed with PBS 0.1% BSA and resuspended with 1:5 PBS diluted 50 µl of sera per 5 mg of conjugated Dynabeads. Binding occurred for 1 h at 37 °C. Beads were washed three times with PBS and elution was performed with 0.2 M Glycine (pH 2.5) subsequently neutralized with 1 M TRIS (pH 8.5) at a 1:0.1 ratio. Resulting samples were loaded on anti-3BNC117 coated plates at a 1 µg ml^{-1} concentration, the fraction of 3BNC117 response was calculated as the standard curve derived concentration of 3BNC117 per 1 µg of purified sera per ml.

ELISPOTs. For ELISPOT assays, cells were collected from the tibia and femur bones by flushing. RBC lysis was performed for 10 min using RBC Lysis Buffer (Biolegend) at room temperature. ELISPOT plates were prepared as previously described[57]. In short, Immobilon P membrane plates (Millipore) were coated with 1 µg ml^{-1} of anti-3BNC117 overnight at 4 °C. Following washing and blocking with 5% BSA in PBS, cells were seeded in dilutions of 1×10^5–1×10^6 per well, in triplicate for each mouse in RPMI 1640 (Biological Industries) supplemented with P/S (Biological Industries), 55 µM β-mercaptoethanol and 10% FCS HI (Sigma). Incubation was performed for 2 days at 37 °C and 5% CO_2. Viability at the time of harvest was commonly 60–80%. After washing, plates were incubated with antimouse IgG (Jackson) for 1 h, washed again and development was performed with an AEC Chromogen Kit (Sigma-Aldrich). Finally, plates were dried and incubated at 4 °C until acquisition on an iSpot ELISPOT reader (AID).

Neutralization assays. Under sterile BSL2/3 conditions, the PSG3 plasmid was cotransfected into HEK293T cells along with JRFL or YU2 HIV envelope plasmids using Lipofectamine 2000 transfection reagent (ThermoFisher Scientific) to produce a single round of infection-competent pseudoviruses representing multiple clades of HIV. HEK293T cells were plated in advance overnight with DMEM medium + 10% FBS + 1% Pen/Strep + 1% L-glutamine. Transfection was done with Opti-MEM transfection medium (Gibco) using Lipofectamine 2000. Fresh medium was added 12 h after transfection. Supernatants containing the viruses were harvested 72 h later. In sterile 96-well plates, 25 µl of virus was immediately mixed with 25 µl of serially diluted (2×) bead protein A/G purified IgG (ThermoFisher) from mouse sera (starting at 500 µg ml^{-1}) and incubated for 1 h at 37 °C to allow for antibody neutralization of the pseudoviruses. 10,000 TZM-bl cells per well (in 50 µl of media containing 20 µg ml^{-1} Dextran) were directly added to the antibody virus mixture. Plates were incubated at 37 °C for 48 h. Following the infection, TZM-bl cells were lysed using 1× luciferase lysis buffer (25 mM Gly-Gly pH 7.8, 15 mM MgSO4, 4 mM EGTA, 1% Triton X-100). Neutralizing ability disproportionate with luciferase intensity was then read on a Biotek Synergy 2 (Biotek) with luciferase substrate according to the manufacturer's instructions (Promega).

qPCR. For copy number quantification of the donor AAV in tissue samples, DNA was extracted from fresh tissues using DNeasy Blood & Tissue Kit (Qiagen) with RNase treatment on-column. Each sample was analyzed for both internal control (Albumin intron[51]) and the donor AAV. For quantification of donor AAV copy number per haploid genome, a standard curve was used. Standards were prepared from a PCR PrimeStar MAX (Takara) reaction using naïve C57BL/6OlaHsd mice genomic DNA for the internal control or donor AAV plasmid for the donor sample and purified using AMPure XP beads (Beckman Coulter) at a 1:1 ratio. A list of primers used for donor and internal control reactions can be found in Supplementary Table 1. Standard curve amplicons were quantified using Qubit (Invitrogen) and serially diluted eight times. For AAV Cas9 quantification RNA was extracted from fresh tissues using RNeasy Mini Kit (Qiagen) with DNAse treatment on-column and postpurification using RQ1 DNAse (Promega). Reverse transcription was performed using RevertAid (ThermoFisher) and random hexamer primers. Data collection and analysis were performed on a StepOnePlus qPCR System (Applied Biosystems) using SYBRGreen (PCR Biosystems). For fold change of AAV titers and *Cas9* relative expression, we used the relative quantity method[58].

Flow cytometry. Collected cells from spleen, bone marrow or blood were resuspended in cell staining buffer (Biolegend) and incubated with 2 µg per 100 µl of human anti-3BNC117 and, where applicable as indicated in the legend, with 1 µg per 100 µl of TruStain FcX (Biolegend) for 10 min, washed and resuspended again in cell staining buffer containing conjugated primary antibodies. A list of antibodies and respective dilutions used in these experiments can be found in Supplementary Table 1. Secondary staining was performed in the dark, for 15 min, with anti-human IgG1 AF647 (Abcam) or anti-human IgK BV421 (Biolegend) or anti-human IgG1 FITC (Biolegend). For primary gp120 staining, cells were incubated with 2 µg per 100 µl of gp120. Then, cells were washed and data acquisition was performed on a CytoFLEX (Beckman Coulter) or Attune NxT (life Technologies) or FACS Aria III (BD Biosciences) for experiments involving cell sorting. Data collection was performed with CytExpert. Data were compiled and analyzed using Kaluza Analysis v.2.1 (Beckman Coulter). Gating strategies can be found in Extended Data Fig. 9.

In vitro B progenitor differentiation. For enrichment of IL7R$^+$ cells, bone marrow from the tibia and femur bones of each mouse was collected at day 97 by flushing (Extended Data Fig. 7a). RBC lysis was performed for 10 min using RBC Lysis Buffer (Biolegend) at room temperature. After washing, cells were resuspended at 2×10^8 cells per ml, in PBS supplemented with 10% FCS (Sigma). PE-conjugated antimouse IL7R (120-048-801, Miltenyi) was added 1/100 and binding was performed on ice for 30 min. Cells were subsequently washed and resuspended at 4×10^8 cells per ml, in PBS supplemented with 10% FCS. Anti-PE microbeads (Miltenyi) were supplemented 1/5 and binding was performed on ice for 30 min. Cell-bead conjugates were once again washed and resuspended at 4×10^7 cells per ml and separated on liquid separation or magnetic separation magnetic columns (Miltenyi).

Following separation, eluate was analyzed for IL7R and CD19 expression (Extended Data Fig. 7e,f) and in vitro differentiation was performed as follows. Cells were seeded in RPMI 1640 (Biological Industries) supplemented with P/S (Biological Industries), 55 µM β-mercaptoethanol, 10% FCS HI (Sigma) and 10 ng ml^{-1} mouse IL7 (Peprotech) at roughly 2×10^6 cells per ml. Three days following seeding (Extended Data Fig. 7b) cells were washed and reseeded in RPMI 1640 (Biological Industries) supplemented with P/S (Biological Industries), 55 µM β-mercaptoethanol, 10% FCS HI (Sigma) and 10 ng ml^{-1} mouse IL4 (Peprotech), 10 µl ml^{-1} lipopolysaccharide (LPS) (Peprotech). Two days following seeding, cells were washed and seeded on 60 gray irradiated CD40LB feeder cells[59] in RPMI 1640 (Biological Industries) supplemented with P/S (Biological Industries), 55 µM β-mercaptoethanol, 10% FCS HI (Sigma), 10 ng ml^{-1} mouse IL4 (Peprotech) and 10 ng ml^{-1} mouse IL21 (Peprotech) at 5×10^5 cells per ml. Two days following seeding, supernatant and cell aliquots were collected for ELISA and flow cytometry, respectively. The rest were washed and reseeded on 60 gray irradiated CD40LB feeder cells in RPMI 1640 (Biological Industries) supplemented with P/S (Biological Industries), 55 µM β-mercaptoethanol, 10% FCS HI (Sigma) and 10 ng ml^{-1} mouse IL21 (Peprotech) at 5×10^5 cells per ml. Finally, 2 d following seeding, cells and supernatant were collected for flow cytometry and ELISA, respectively.

Hematopoietic stem and progenitor enrichment and adoptive transfer. For bone marrow Lin$^-$ hematopoietic stem and progenitor cells enrichment, cells were collected from the tibia and femur bones of female CD45.2 C57BL/6JOlaHsd mice at day 97 by flushing (Extended Data Fig. 8a). RBC lysis was performed for 10 min using RBC Lysis Buffer (Biolegend) at room temperature. Following washing, cells were magnetically enriched using the Mouse Lineage Cell Depletion Kit (Miltenyi) using liquid separation or magnetic separation magnetic columns (Miltenyi), according to the manufacturer's instructions.

Following separation, flow through aliquots were analyzed for Lin and B220 expression. The rest of the cells were adoptively transferred into mice as with an adaptation of a previously described protocol[60]. In short, recipient female, 8 weeks old, CD45.1 C57BL/6JOlaHsd mice were sublethally irradiated at 150 cGy and, the following day, received 6×10^5 cells per 100 µl per mouse in PBS by retro-orbital injections.

In vitro FcR loading. Primary bone marrow CD11b were collected 5 days following activation and 2×10^6 cells were further cultured in FBS/granulocyte-macrophage colony-stimulating factor (GMCSF) supplemented DMEM with 2 µg ml^{-1} of purified mouse IgK/IgG2a 3BNC117. Cells were collected after 20 min and then FcRX blocked before analysis by flow cytometry using the anti-3BNC117 anti-idiotype antibody.

For primary splenic lymphocytes, cells were collected from naïve mice and were cultured in FBS supplemented RPMI with 2 µg ml^{-1} of purified mouse IgK/IgG2a 3BNC117. Cells were collected after 20 min and then FcRX blocked before analysis by flow cytometry using the anti-3BNC117 anti-idiotype antibody.

In vitro engineering of B cells. CRISPR–Cas9 RNP electroporations and AAV transductions of B cells was performed as described previously[7]. In short, total splenic lymphocytes were collected from spleens of naïve mice and activated in LPS and IL-4 for electroporation (Neon, ThermoFisher) the following day. For anti-idiotype specificity, AAV-DJ transduction was performed at 50,000 multiplicity of infection (MOI) and for AID independent integrations at 10,000 or 100,000 MOI, as indicated in the figures.

Ex vivo engineering of CD11b cells. Total bone marrow cells were extracted by flushing tibia and femur. Cells were cultured in DMEM (Biological Industries) supplemented with 15% FBS (Biological Industries) and 50 ng ml^{-1} of GMCSF (Peprotech) to activate and proliferate CD11b cells[61]. Five days following activation, 1×10^6 cells were electroporated with pregenerated complexes of 20 pmol spCas9 (IDT) and 25 pmol sgRNA (IDT) in buffer T at 1,600 V, 20 ms, 1 pulse. Immediate AAV-DJ transduction was performed at 200,000 MOI. Cells were subsequently cultured for 1 day at 1×10^6 cells per ml in GMCSF/FBS supplemented DMEM and for an additional 5 d without GMCSF before analysis flow cytometry.

Nucleic acid manipulations. For RT–PCR demonstrating *3BNC117* gene integration into the *IgH* locus, RNA was extracted from sorted engineered B cells (3BNC117$^+$, CD4$^-$, CD19$^+$) on a FACS BD Aria III (BD Biosciences). As a positive control, we used in vitro engineered mouse splenic lymphocytes, as described previously[7]. In short, mouse splenic lymphocytes were activated with 10 µg ml^{-1} LPS (Santa-Cruz Biotechnology) and 10 ng ml^{-1} IL-4 (Peprotech) for 24 h, electroporated by CRISPR–Cas9 RNP using a Neon Electroporation System (Invitrogen) and transduced at 50,000 MOI of the donor AAV-DJ vector. For RNA extraction, we used RNeasy Mini Kit (Qiagen) with DNAse treatment on-column and reverse transcription was performed using RevertAid (ThermoFisher) and Oligo dT primers. PCR on the resulting complementary DNA was performed for 35 cycles using PrimeStar MAX (Takara). Then, a seminested PCR was performed using PrimeStar MAX (Takara) for 35 cycles. A list of primers used for these reactions may be found in Supplementary Table 1. Following each PCR, resulting amplicons were analyzed by Agarose gel electrophoresis as compared to a standardizing ladder (Hylabs, GeneDireX 1 Kb plus DNA ladder RTU or 100 bp DNA ladder H3 RTU) and total reactions were purified using AMPure XP beads (Beckman Coulter) at a 1:1 ratio. Purified amplicons were Sanger sequenced at the DNA Sequencing Unit, Tel Aviv University and presented alignment of the chromatograms was performed using SnapGene (GSL Biotech).

For TIDE analysis of on-target cleavage, gDNA from tissues was extracted from fresh tissues using Gentra PureGene Tissue Kit (Qiagen). PCR was performed for 35 cycles using PrimeStar MAX (Takara). Primers used for these reactions can be found in Supplementary Table 1. For the control samples, three independent PCR were performed on independent gDNA samples, collected from splenic tissue of naïve C57BL/6OlaHsd mice. Resulting amplicons were purified using AMPure XP

beads (Beckman Coulter) at a 1:1 ratio. Purified amplicons were Sanger sequenced at the DNA Sequencing Unit, Tel Aviv University. For each sample, multiple sequencing reactions were performed using either primers. Then, samples were compared using TIDE (https://tide.nki.nl/)[62]. For control samples, we performed reciprocal sample comparisons from the independent initial PCR reactions. For all samples, along with the CMV expressed Cas9, mice received the donor vector. Along with the SFFV or CD19 expressed Cas9, mice received the donor^{gRNA} vector. Control samples come from naïve splenic lymphocytes (Fig. 6i).

Anti-Idiotipic to 3BNC117 scFvs were generated by phage display[63]. Candidates were cloned into pcDNA3.1 vectors with the human kappa and IgG1 heavy chain. In short, antibodies were produced by transfection of both antibody chains into Expi293F cells (Gibco) by Expifectamine (Gibco) and purified using MabSelect (GE Healthcare) as previously described[7]. Specificity and sensitivity of the antibody were verified in vitro using primary B cells engineered, as described previously[7], to express one of the three bNAbs, 3BNC117, VRC01 or 10-1074. Both 3BNC117 and VRC01 bind to the CD4 binding site. However, only 3BNC117 binds to its anti-idiotype (Extended Data Fig. 10).

For reverse transcription PCR of ex vivo engineered cells, RNA was extracted, two days following treatment, from 5×10^5 splenic lymphocytes or 6 d following treatment from 5×10^5 GMCSF activated bone marrow cells. RNA extraction was performed using Quick-RNA micro prep (Zymo Research) without DNAse treatment. Reverse transcription was performed using RevertAid (ThermoFisher) and Oligo dT primers. PCR of exon–exon junctions on the resulting cDNA was performed for 30 cycles using HS Taq Mix (PCRBio), a list of primers used for these reactions can be found in Supplementary Table 1.

Statistics. Statistical analyses were performed on distinct samples using Prism (GraphPad). For the area under the curve (AUC), in each group, the mean AUC and s.d. were calculated and these values were compared by *t*-test. All *t*-tests were performed as two-tailed. For the TIDE analysis, each comparison between a control sample and an independently produced PCR reaction from three independent mice were used. Each figure legend denotes the statistic used, central tendency and error bars.

Reporting summary. Further information on research design is available in the Nature Research Reporting Summary linked to this article.

Data availability

Data are available in the main text, in the Extended Data figures and Supplementary Data and materials. Illumina sequencing data can be accessed in the SRA database under accession code PRJNA706552. Source data are provided with this paper.

References

51. Barzel, A. et al. Promoterless gene targeting without nucleases ameliorates haemophilia B in mice. *Nature* **517**, 360–364 (2015).
52. Magoč, T. & Salzberg, S. L. FLASH: fast length adjustment of short reads to improve genome assemblies. *Bioinformatics* **27**, 2957–2963 (2011).
53. Lee, H., Chang, H. Y., Cho, S. W. & Ji, H. P. CRISPRpic: fast and precise analysis for CRISPR-induced mutations via prefixed index counting. *NAR Genom. Bioinform.* **2**, lqaa012 (2020).
54. Langmead, B. & Salzberg, S. L. Fast gapped-read alignment with Bowtie 2. *Nat. Methods* **9**, 357–359 (2012).
55. Stern, A. et al. Selecton 2007: advanced models for detecting positive and purifying selection using a Bayesian inference approach. *Nucleic Acids Res.* **35**, 506–511 (2007).
56. Benjamini, Y. & Hochberg, Y. Controlling the false discovery rate: a practical and powerful approach to multiple testing. *J. R. Stat. Soc. Ser. B* **57**, 289–300 (1995).
57. Wieland, A. et al. Defining HPV-specific B cell responses in patients with head and neck cancer. *Nature* **597**, 274–278 (2020).
58. Livak, K. J. & Schmittgen, T. D. Analysis of relative gene expression data using real-time quantitative PCR and the $2^{-\Delta\Delta c_T}$ method. *Methods* **25**, 402–408 (2001).
59. Nojima, T. et al. In-vitro derived germinal centre B cells differentially generate memory B or plasma cells in vivo. *Nat. Commun.* **2**, 411–465 (2011).
60. Ferrari, S. et al. Efficient gene editing of human long-term hematopoietic stem cells validated by clonal tracking. *Nat. Biotechnol.* **38**, 1298–1308 (2020).
61. Santana-Magal, N. et al. Melanoma-secreted lysosomes trigger monocyte-derived dendritic cell apoptosis and limit cancer immunotherapy. *Cancer Res.* **80**, 1942–1956 (2020).
62. Brinkman, E. K., Chen, T., Amendola, M. & Van Steensel, B. Easy quantitative assessment of genome editing by sequence trace decomposition. *Nucleic Acids Res.* **42**, e168 (2014).
63. Bitton, A., Nahary, L. & Benhar, I. in *Phage Display: Methods and Protocols* (eds. Hust, M. & Lim, T. S.) 349–363 (Springer, 2018).

Acknowledgements

We thank the Veterinary Service Center, Tel Aviv University for animal husbandry. The IDRFU, Genomic Research Unit and SICF units, Tel Aviv University for logistic support and council. We also thank L. Vardi, M. Gelbart, H. Kobo, D. Burstein, I. Benhar, N. Freund, M. Kay, T. Akriv and N. Gritsenko for reagents and feedback. This research was funded by the Varda and Boaz Dotan donation (A.B.), the H2020 European Research Council grant no. 759296 570 (A.B.) and the Israel Science Foundation grant nos. 1632/16, 2157/16 and 2876/21 (A.B.), The Bill and Melinda Gates Foundation grant no. OPP1183956 (J.E.V.), National Institutes of Health grant nos. R01 AI167003-01 (A.B.) AI128836 and R01 AI073148 (D.N.), Edmond J. Safra Center for Bioinformatics fellowship (T.K. and A.S.), St. Jude Children's Research Hospital and ALSAC, National Institutes of Health Office Of The Director, Somatic Cell Genome Editing initiative grant no. U01AI157189 (S.Q.T.), the Gertner Institute Scholarship, the Yoran Institute Scholarship and the SAIA Foundation (A.D.N.). The content is solely the responsibility of the authors and does not necessarily represent the official views of the National Institutes of Health.

Author contributions

A.D.N. designed, performed and analyzed the study. C.R.L. performed CHANGE-seq; S.Q.T. supervised CHANGE-seq experiments. N.Z. and T.K. performed bioinformatical analyses. A.S. and R.R.-A. supervised the bioinformatical analyses. N.Z., M.H.-F. and I.R. helped with sample processing. Y.R. helped with vector design and cloning. D. Nataf and I.D. designed the B cell progenitor enrichment. M.T. and D.H. performed neutralization assays. D. Nemazee and J.E.V. supervised neutralization assays. I.D. contributed to supervising the study. Y.C. helped with experimental design. A.D.N. and A.B. drafted and revised the manuscript. A.B. conceptualized and supervised the study.

Competing interests

A.D.N., D. Nataf, M.H.-F., I.D. and A.B. are listed as inventors on patent applications covering B cell engineering. A.D.N. and A.B. have an equity stake in and receive monetary compensation from Tabby Therapeutics Ltd, a B cell engineering company. S.Q.T. is a coinventor on patents covering the CHANGE-seq method. S.Q.T. is a member of the scientific advisory boards of Kromatid, Inc. and Twelve Bio. The other authors declare no competing interests.

Additional information

Extended data are available for this paper at https://doi.org/10.1038/s41587-022-01328-9.

Supplementary information The online version contains supplementary material available at https://doi.org/10.1038/s41587-022-01328-9.

Correspondence and requests for materials should be addressed to Adi Barzel.

Peer review information *Nature Biotechnology* thanks the anonymous reviewers for their contribution to the peer review of this work.

Reprints and permissions information is available at www.nature.com/reprints.

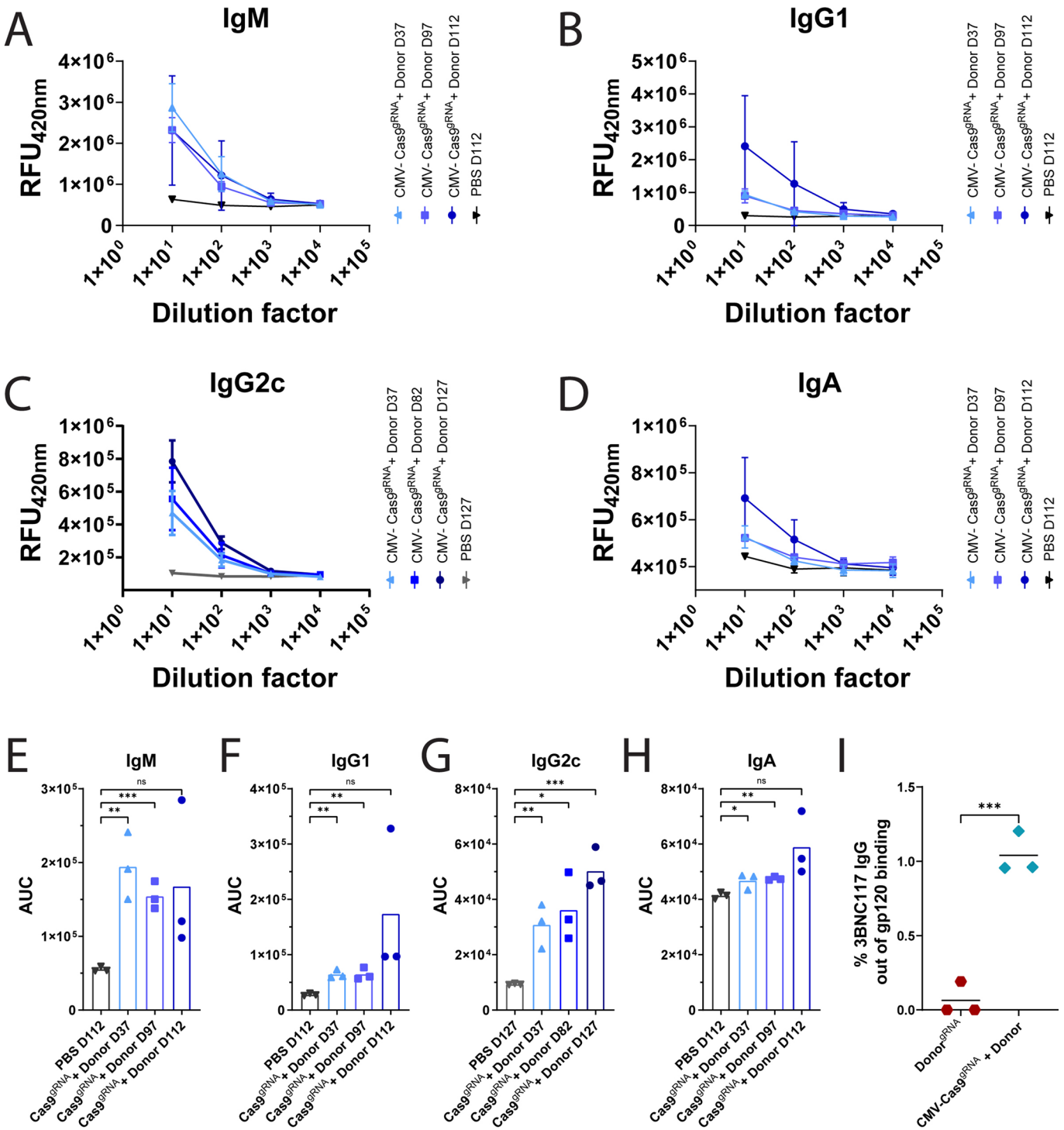

Extended Data Fig. 1 | Multiple isotypes of the 3BNC117 antibody are expressed by engineered B cells. a–d. ELISA for each isotype. **a**. IgM, **b**. IgG1, **c**. IgG2c and **d**. IgA. All samples come from the CMV-Cas9^{gRNA} + donor injected mice at different time points, as indicated in each legend. Mean and SD are indicated. n = 3 biologically independent animals. **e,f**. Area under the curve (AUC) for A-D. **e**. IgM, ns; pv = 0.1288, ***; pv = 0.0008, **; pv = 0.0062, **f**. IgG1, ns; pv = 0.131 and from top to bottom as presented in the graph, **; pv = 0.0044 and pv = 0.0013, **g**. IgG2c, ***; pv = 0.0007, *; pv = 0.0195, **; pv = 0.0098, **h**. IgA, ns; pv = 0.0587, **; = pv = 0.0013, *; pv = 0.0403, for two-sided unpaired t-test. n = 3 biologically independent animals. For A-H, sample collection day is indicated. Mean values are indicated. **i**. Fraction of 3BNC117 IgG titers as quantified by ELISA using purified gp120 binding sera from donor injected mice immunized with gp120, at day 37. ***; pv = 0.0007 for two-sided unpaired t-test. n = 3 biologically independent samples. Mean values are indicated.

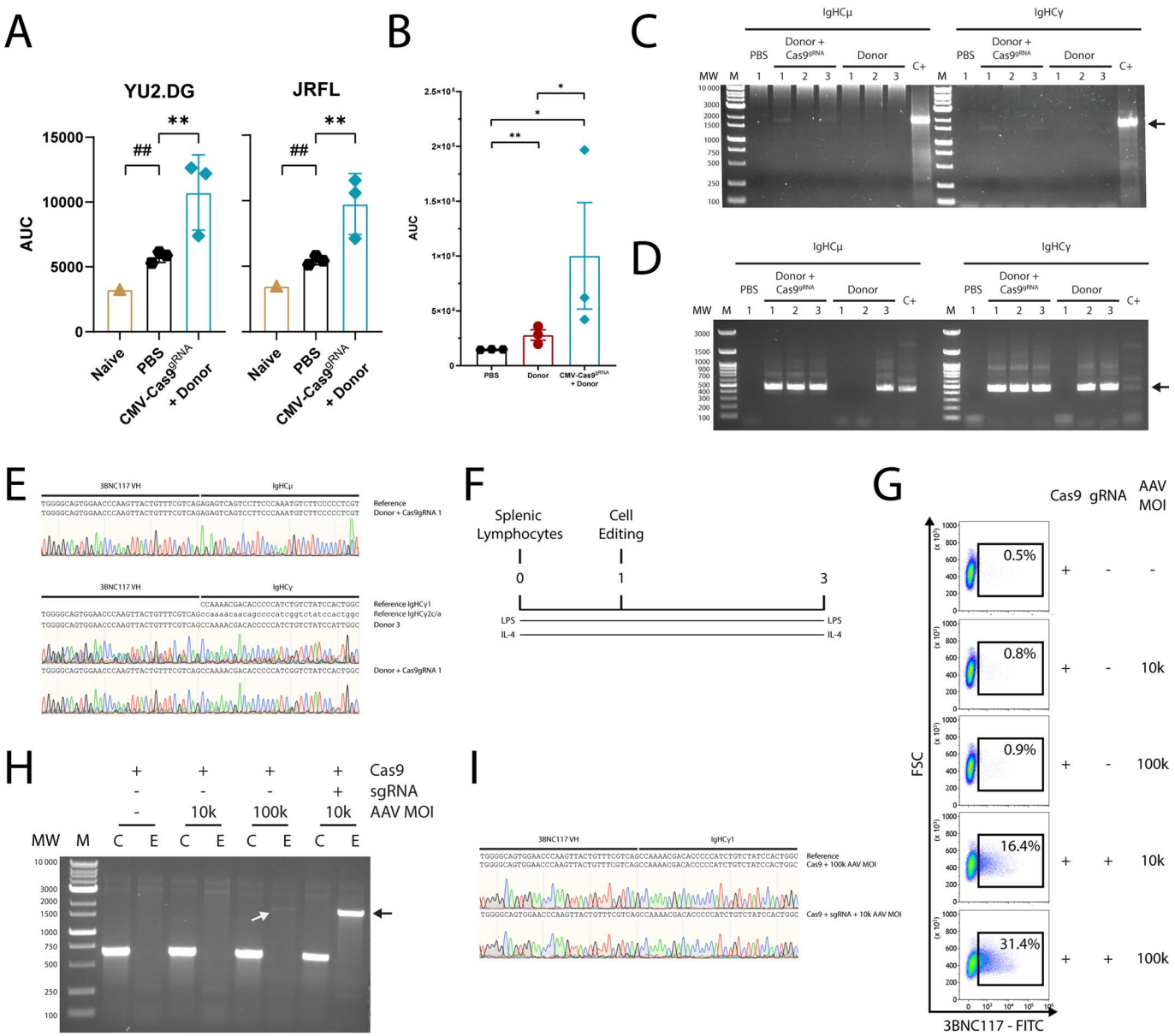

Extended Data Fig. 2 | bNAb genomic integration, sera titers and neutralization as a function of immunizations and co-injection of the CRISPR-Cas9 vector. a. Area under the Curve (AUC) of Fig. 2d for YU2.DG (left) and JRFL (right) **; pv = 0.0036 (YU2.DG) and pv = 0.005 (JRFL) for unpaired t-test for CMV-Cas9gRNA + donor to PBS comparison and ##; pv = 0.0072 (YU2.DG) and pv = 0.0063 (JRFL) for one-sample t-test for Naïve to PBS comparison. n = 3 for CMV-Cas9gRNA + donor and PBS. Naïve sample is from a single, non-immunized, non-AAV-injected mouse. Mean values ± SD are indicated. **b**. Area under the curve (AUC) of Fig. 2c. From top to bottom, *; pv = 0.0185 and pv = 0.0103, **; pv = 0.0036 for two-sided unpaired t-test. n = 3 biologically independent animals. Mean values ± SEM are indicated. **c**. RT-PCR on RNA from sorted, 3BNC117^{+}, CD19^{+}, CD4^{-} blood lymphocytes from day 37. Here, we used a reverse primer in a membranal exon of either *IgHCμ* or *IgHCγ* (all subtypes) and a forward primer on the V_H of the coded 3BNC117. Numbers indicate different mice, injected with either a) PBS, b) the donor vector and the CMV-Cas9^{gRNA} vector, or c) the donor vector only, as indicated above the gels. Control sample (C+) comes from *in-vitro* engineered primary mouse splenic lymphocytes, as described previously[7]. Ladder sizes are indicated on the left. Arrow indicates the expected amplicon size. For each group, experiment was reproduced 3 times with independent samples, as indicated by the numbers. Molecular weight markers (M) and their respective size in base pairs (MW) are indicated. **d**. Total DNA from the previous reaction as in (C) was purified and a semi-nested PCR with the same forward primer and a reverse primer on the CH1 of the respective constant domains. Ladder sizes are indicated on the left. Arrow indicates the expected amplicon size. For each group, experiments were reproduced 3 times with independent samples. Molecular weight markers (M) and their respective size in base pairs (MW) are indicated. **e**. Sanger sequencing alignment and chromatogram of the purified amplicon from the previous step. Reference sequences are indicated above. For the *IgHCγ*, each subtype reference is indicated. Sequencing of the *IgHCμ* amplicon of donor 3 has failed. **f**. Experimental design for (G-I). Splenic lymphocytes were activated with LPS and IL-4 and engineered, ex vivo, by AAV transduction and Cas9 electroporation with or without a gRNA. **h**. Flow cytometry of engineered splenic lymphocytes two days following treatment. Pregated on live, singlets. FcR block was used in the staining. Engineering parameters are indicated above each plot. **h**. EtBr gel electrophoresis showing products of an RT-PCR reaction with RNA from cells two days following treatment as in (F). For each sample, a control (C) reaction was performed amplifying the endogenous *IgHG1* cDNA. Ladder sizes are indicated on the left. Arrow indicates the expected amplicon size. The experiment was reproduced once, with similar results. Molecular weight markers (M) and their respective size in base pairs (MW) are indicated. **i**. Sanger sequencing of the previous amplicons, confirming the integration.

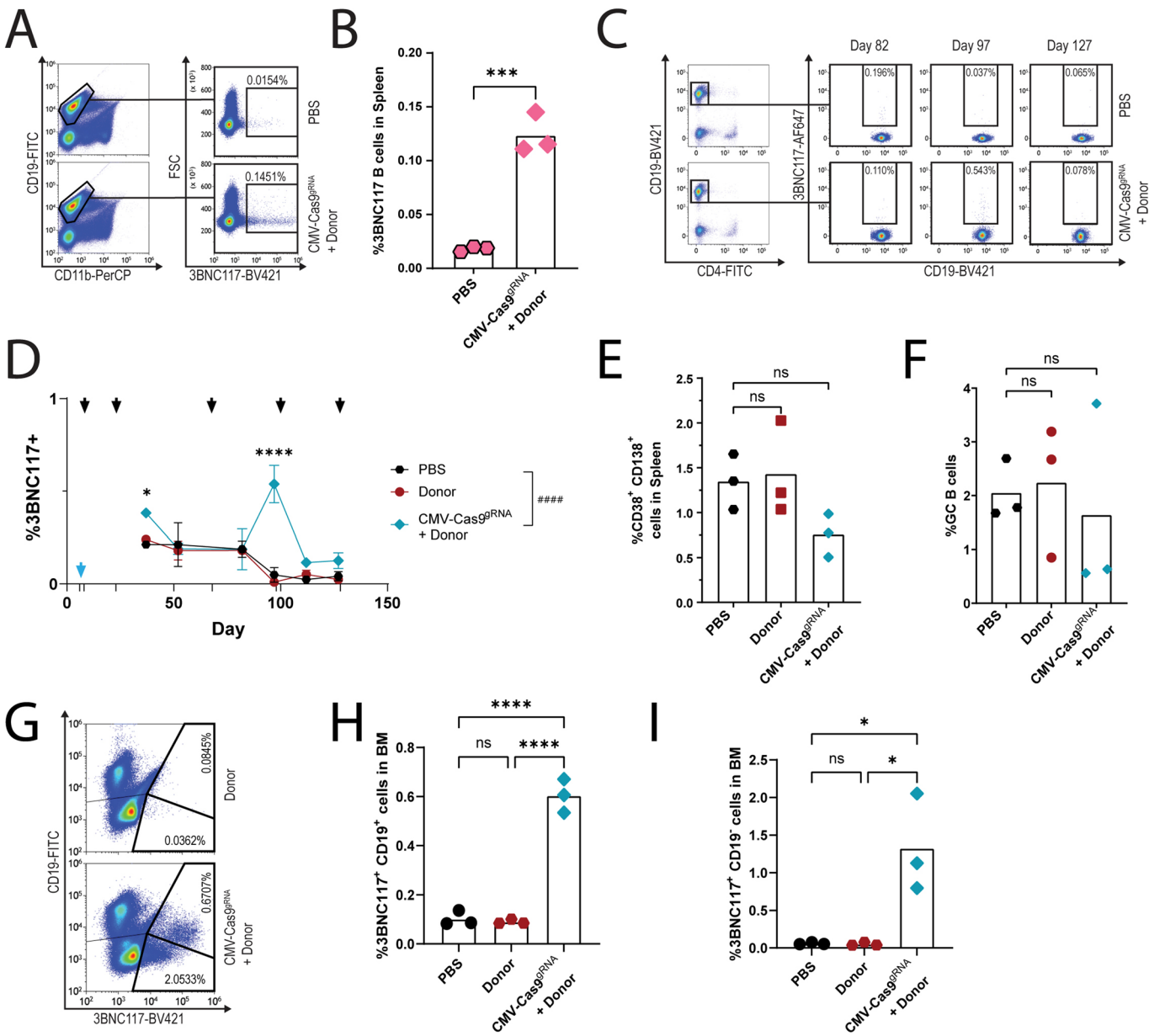

Extended Data Fig. 3 | Detection of engineered B cells in the spleen, the blood and the bone marrow. a. Flow cytometry plots demonstrating 3BNC117 expression among CD19⁺ CD11b⁻ cells in the spleen at day 82 of 2CC immunized mice. Pregated on live, singlets. FcR block was used in the staining. **b**. Quantification of B. ***; pv = 0.0006 for two-sided unpaired t-test. **c**. Flow cytometry plots demonstrating 3BNC117 expression among blood B cells (CD19⁺, CD4⁻). **d**. Quantification of blood 3BNC117-expressing cells over time. The black arrows indicate immunizations and the blue arrow indicates AAV injection. ####; pv < 0.0001 for Two-Way ANOVA comparison between groups and *; pv = 0.0133, ****; pv < 0.0001 Two-Way ANOVA with Šidák's multiple comparison for time points comparison to PBS. For each group, each line represents the mean ±SD of n = 3 biologically independent mice. **e**. Quantification of total CD38⁺ CD138⁺ in spleens of recipient mice as in Fig. 3a. From top to bottom: ns; pv = 0. 2380 and pv = 0.9907 for One-Way ANOVA with Tukey's multiple comparisons test. **f**. Quantification of total GL7⁺ CD95⁺ cells as in Fig. 3e. From top to bottom: ns; pv = 0.9857 and pv = 0.9985 for One-Way ANOVA with Tukey's multiple comparisons test. **g**. Flow cytometry plots demonstrating the presence of 3BNC117-expressing B cells in the bone marrow. **h-i**. Quantification of G. ns; pv = 0.9965, ****; pv < 0.0001 (G) and from top to bottom: ns; pv > 0.9999, *; pv = 0.0387 and pv = 0.0372 (H) for One-Way ANOVA with Tukey's multiple comparison.

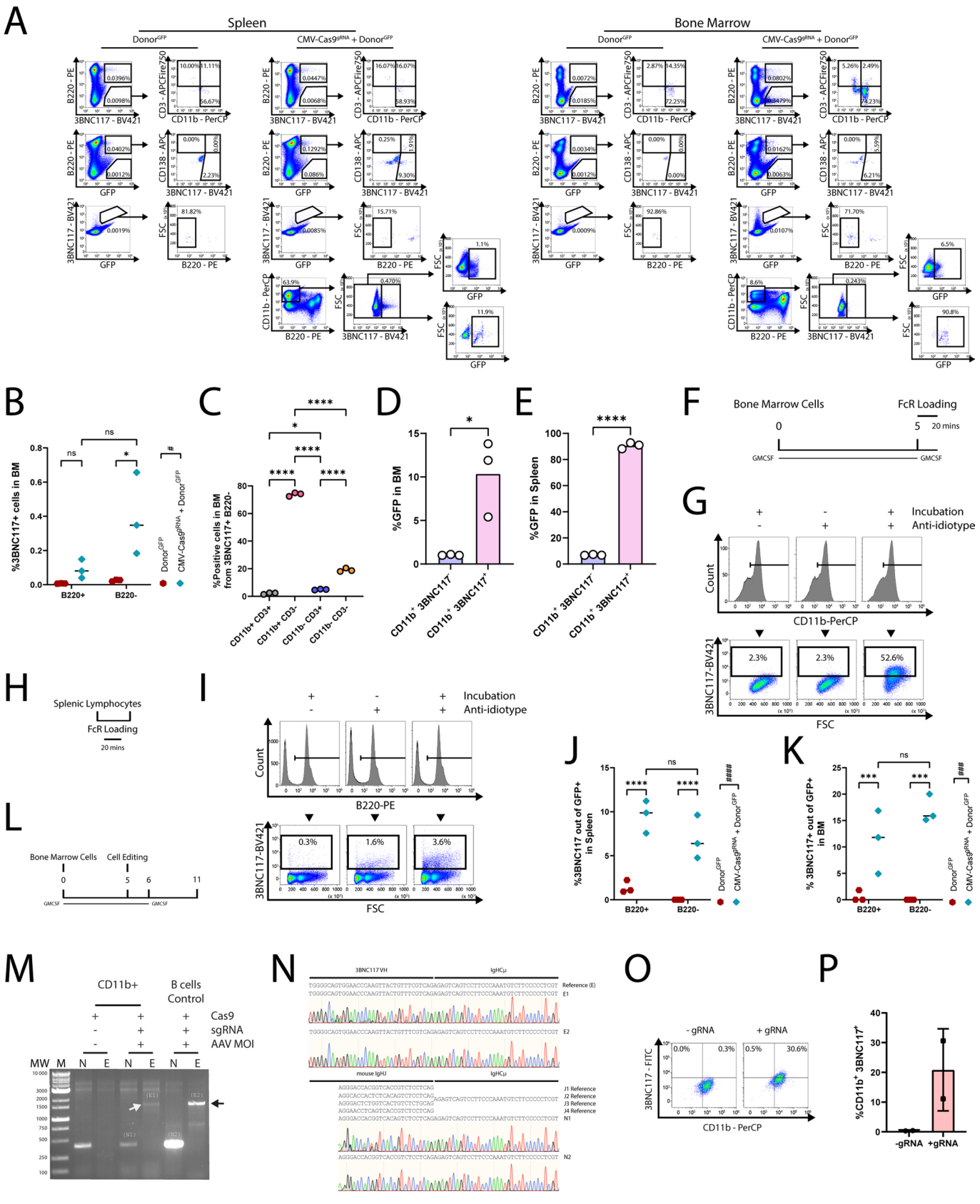

Extended Data Fig. 4 | See next page for caption.

Extended Data Fig. 4 | Assessing expression of the transgene in different subsets of cells. a. Flow cytometry examples for Fig. 5c-g and Extended Data Fig. 3b-e, j-k. **b**. Quantification of 3BNC117$^+$ cells in bone marrow. #; pv = 0.0129 for Two-Way ANOVA and *; pv = 0.0255 for Two-Way ANOVA with Tukey's multiple comparison. **c**. Quantification of the indicated populations from 3BNC117$^+$ B220$^-$ cells in the bone marrow. *; pv = 0.0335, **** = pv < 0.0001 for One-Way ANOVA with Tukey's multiple comparison. **d,e**. Quantification of GFP$^+$ cells from the CD11b$^+$ 3BNC117$^+$ or CD11b$^+$ 3BNC117$^-$ populations in the bone marrow (D) or spleen (E). *; pv = 0.0214, **** = pv <0.0001 for unpaired two-tailed t-test. Mean values are indicated. **f**. Experimental scheme for (G). Bone marrow cells were collected and activated in the presence of GMCSF. 5 days later, cells were cultured in the presence of purified mouse 3BNC117 for FcR presentation and then collected for analysis by flow cytometry. **g**. Analysis by flow cytometry, using the anti-3BNC117 anti-idiotypic antibody, of bone marrow cells activated by GMCSF and subsequently cultured with 3BNC117. Experimental conditions are indicated above. Pre-gated on CD11b, live, singlets. **h**. Experimental scheme for (I). Splenic Lymphocytes are collected from mice and cultured with purified mouse 3BNC117. Next, cells are collected for Flow Cytometry. **i**. Analysis by flow cytometry, using the anti-3BNC117 anti-idiotypic antibody, of splenic lymphocytes cultured with 3BNC117. Experimental conditions are indicated above. Pre-gated on B220$^+$, live, singlets. **j-k**. Quantification of 3BNC117$^+$ cells from GFP$^+$ cells in the spleen (J) ####; pv < 0.0001 for Two-Way ANOVA and ns; pv = 0.1748, ****; pv < 0.0001 for Two-Way ANOVA with Tukey's multiple comparison or bone marrow (K) ###; pv = 0.001 for Two-Way ANOVA and ns; pv = 0.6177, and from left to righ: ***; pv = 0.0005 and pv = 0.0005 for Two-Way ANOVA with Tukey's multiple comparison. BM = bone marrow. **l**. Experimental scheme of *in-vitro* engineering of primary GMCSF activated bone marrow cells for (M-N). **m**. EtBr gel electrophoresis showing the product of an RT-PCR reaction of RNA from activated bone marrow cells, six days following treatment as in (L). For each sample, two reactions were performed (N or E). N amplifies endogenous IgHCμ mRNA. E amplifies the transgene mRNA joined by splicing to the IgHCμ exons following engineering. Indicated labeling of the amplicons (E1, E2, N1 and N2) performed for reference in (N). The experiment was performed once with expected results. Molecular weight markers (M) and their respective size in base pairs (MW) are indicated. **n**. Sanger sequencing of the amplicons, confirming correct integration. Amplicons are annotated E1, E2, N1 and N2 as in (M). **o**. Flow cytometry example of engineered GMCSF activated primary bone marrow cells. Pre-gated on B220$^-$, live, singlets. **p**. quantification of O. Control cells are cells transduced with the AAV and electroporated only with the spCas9, without the sgRNA (-gRNA). For A-P and Fig. 3, FcR block was used in the staining. For each group, n = 2 biologically independent samples.

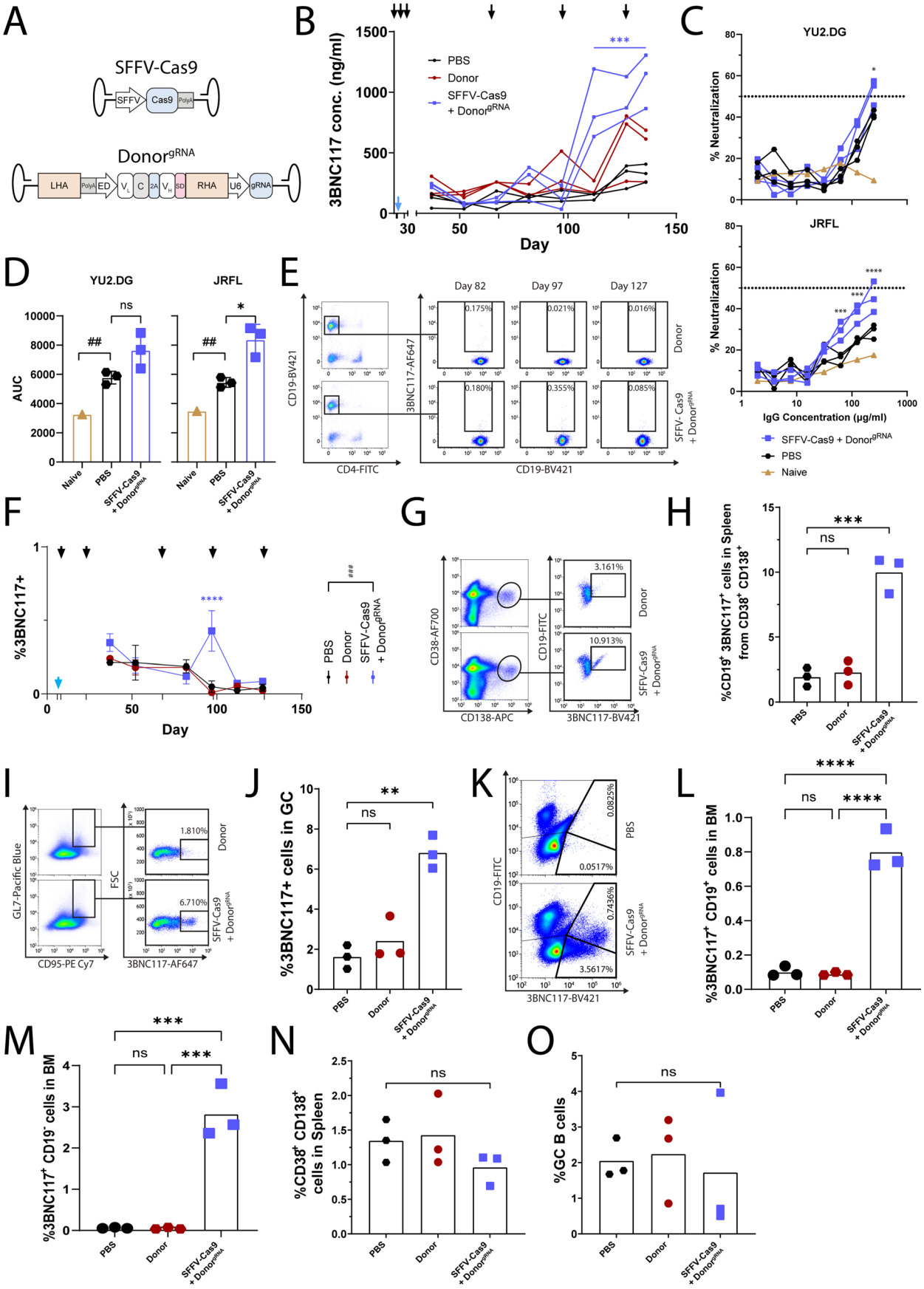

Extended Data Fig. 5 | See next page for caption.

Extended Data Fig. 5 | Engineering B cells with the sgRNA coded on the donor AAV. a. Vector maps of the AAVs coding for the donor^{gRNA} and the SFFV-Cas9. **b**. 3BNC117 IgG titers as quantified by ELISA over time in the SFFV-Cas9 + donor^{gRNA} group. The black arrows indicate immunizations and the blue arrow indicates AAV injection. Each line represents a mouse. ***; pv = 0.0005 for Two-Way ANOVA comparing the SFFV-Cas9 + donor^{gRNA} group to the donor group. n = 3 biologically independent mice. In this panel, the PBS and donor control groups are the same as for Fig. 2B. **c**. Transduction neutralization of TZM.bl cells by the YU2.DG (top) and JRFL (bottom) HIV pseudoviruses in the presence of day 136 sera IgGs. Neutralization is calculated as percent reduction from maximal luminescence per sample. The PBS control received immunizations, while the naïve control represents serum IgG from an untreated mouse. ns = non-significant, *; pv = 0.0462 and from top to bottom: ***; pv = 0.0007 and pv = 0.0004, ****; pv < 0.0001, Two-Way ANOVA with Šidák's multiple comparison for time points comparison to PBS. **d**. Area under the Curve (AUC) for C. for YU2.DG and JRFL. ns; pv = 0.0667 (YU2.DG) and *; pv = 0.0103 (JRFL) for two-sided unpaired t-test for CMV-Cas9gRNA + donor to PBS comparison and ##; pv = 0.0097 (YU2.DG) and pv = 0.0078 (JRFL) for two-sided one-sample t-test for naïve to PBS comparison. n = 3 for CMV-Cas9gRNA + donor and PBS. Naïve sample from a single, non-immunized, non-AAV-injected mouse. In C-D, the PBS and control group is the same as for Fig. 2c and Extended Data Fig. 2a. Mean values ± SD are indicated. **e**. Representative flow cytometry analysis of 3BNC117^{+}, CD19^{+}, CD4^{-} blood lymphocytes over time in the SFFV-Cas9 + donor^{gRNA} group. **f**. Quantification of E. The black arrows indicate immunizations and the blue arrow indicates AAV injection. ###; pv = 0.0006 for Two-Way ANOVA comparison between groups and ****; pv < 0.0001 for Two-Way ANOVA with Šidák's multiple comparison for time points comparison to PBS. For each group, each line represents the mean ±SD of n = 3 biologically independent mice. **g**. Representative flow cytometry analysis of 3BNC117^{+}, CD19^{+}, CD38^{+}, CD138^{+} plasmablasts in the spleens of the SFFV-Cas9 + donor^{gRNA} group at day 136. **h**. Quantification of G. Mean is indicated by the bars. ns; pv = 9892, ***; pv = 0.0005, one-way ANOVA with Tukey's multiple comparison. **i**. Representative flow cytometry analysis of GL7^{+}, Fas/CD95^{+} GC B cells in the spleens of the SFFV-Cas9 + donor^{gRNA} group at day 136. **j**. Quantification of I. Mean is indicated by the bars. ns; pv = 0.8916, **; pv = 0.0075, one-way ANOVA with Tukey's multiple comparison. **k**. Representative flow cytometry analysis of 3BNC117^{+} cells in total bone marrow (BM) of the SFFV-Cas9 + donor^{gRNA} group at day 136. **l**. Quantification of 3BNC117^{+} CD19^{+} cells, ns; pv = 0.9965 and ****; pv < 0.0001 and **m**. Quantification of 3BNC117^{+} CD19^{-} cells, ns; pv > 0.9999 and from top to bottom: ***; pv = 0.0003 and pv = 0.0003. Mean is indicated by the bars. One-way ANOVA with Tukey's multiple comparison. **n-o**. Assessing overall immune homeostasis. Quantification by flow cytometry of total CD38^{+} CD138^{+} plasmablasts in spleen (N) ns; pv = 0.5622, total GL7^{+}, Fas^{+} GC B cells in the spleen (O), at day 136 ns; pv = 0.9926. Mean is indicated by the bars.One-way ANOVA with Tukey's multiple comparison. For E-O, the PBS and donor control groups are the same as for Fig. 3 and Extended Data Fig. 3.

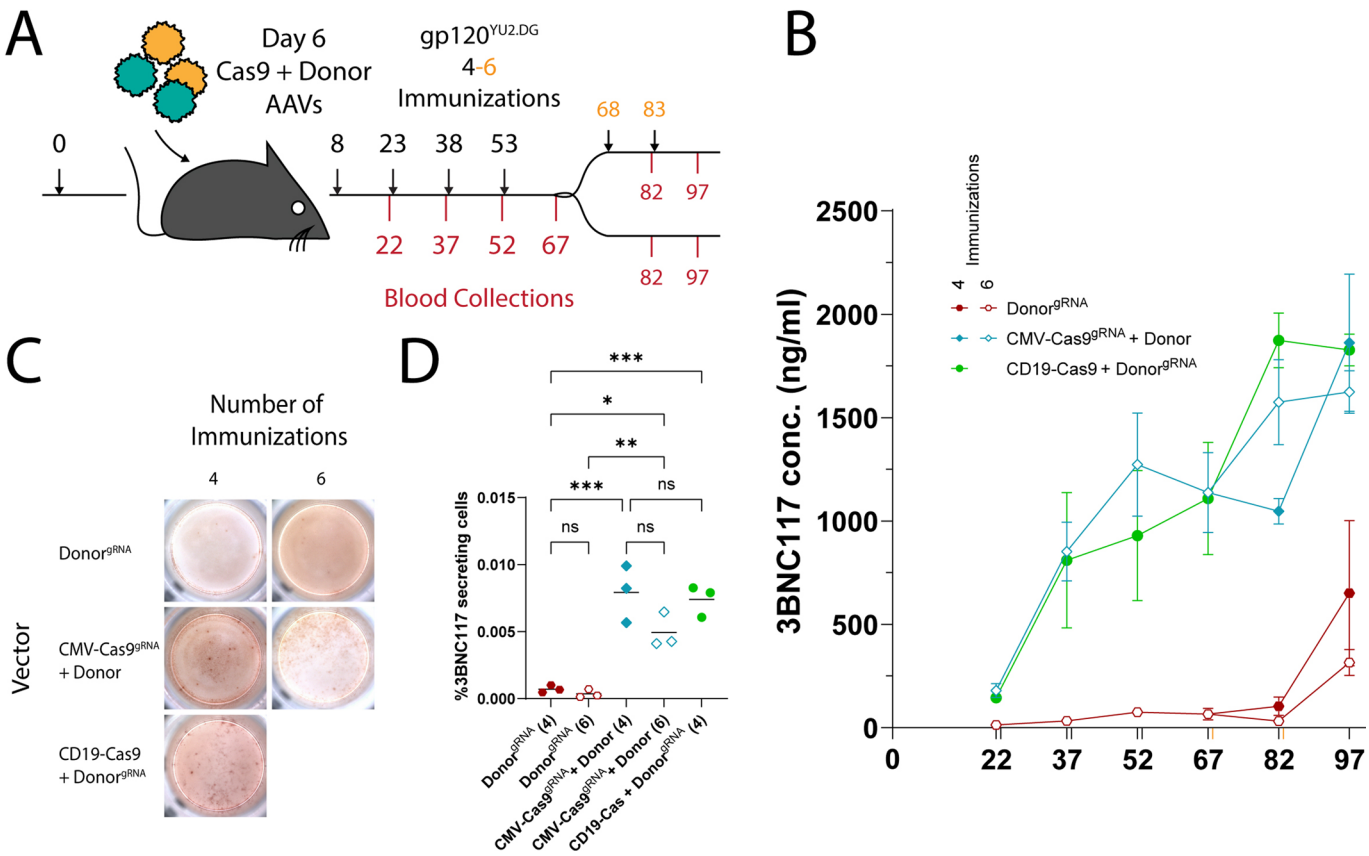

Extended Data Fig. 6 | Long-term persistence of serum antibodies and antibody-secreting cells in the bone marrow. a. Experimental design. Here, all mice were immunized 4 times (days 8,23,38 and 53) and selected groups received 2 additional immunizations on days 68 and 83. **b**. 3BNC117 IgG titers as quantified by ELISA over time. For each group, each line represents the mean ±SD between day 22 and day 67 represents n = 6 for biologically independent mice and n = 3 for day 67 to 97. **c-d**. Representative ELISPOT experiments (C) and quantification (D) of 3BNC117-secreting cells from the bone marrow of mice of the indicated groups. Numbers in parentheses represent the number of immunizations. From top to bottom followed by left to right, ns; pv = 0.9844 and pv = 0.9963 and pv = 0.0884, *; pv = 0.0135, **; pv = 0.008, ***; pv = 0.0005 and pv = 0.0003 for One-Way ANOVA with Tukey's multiple comparison. Mean values are indicated. Part of the data presented in panels B-D is presented also in Fig. 6c–e.

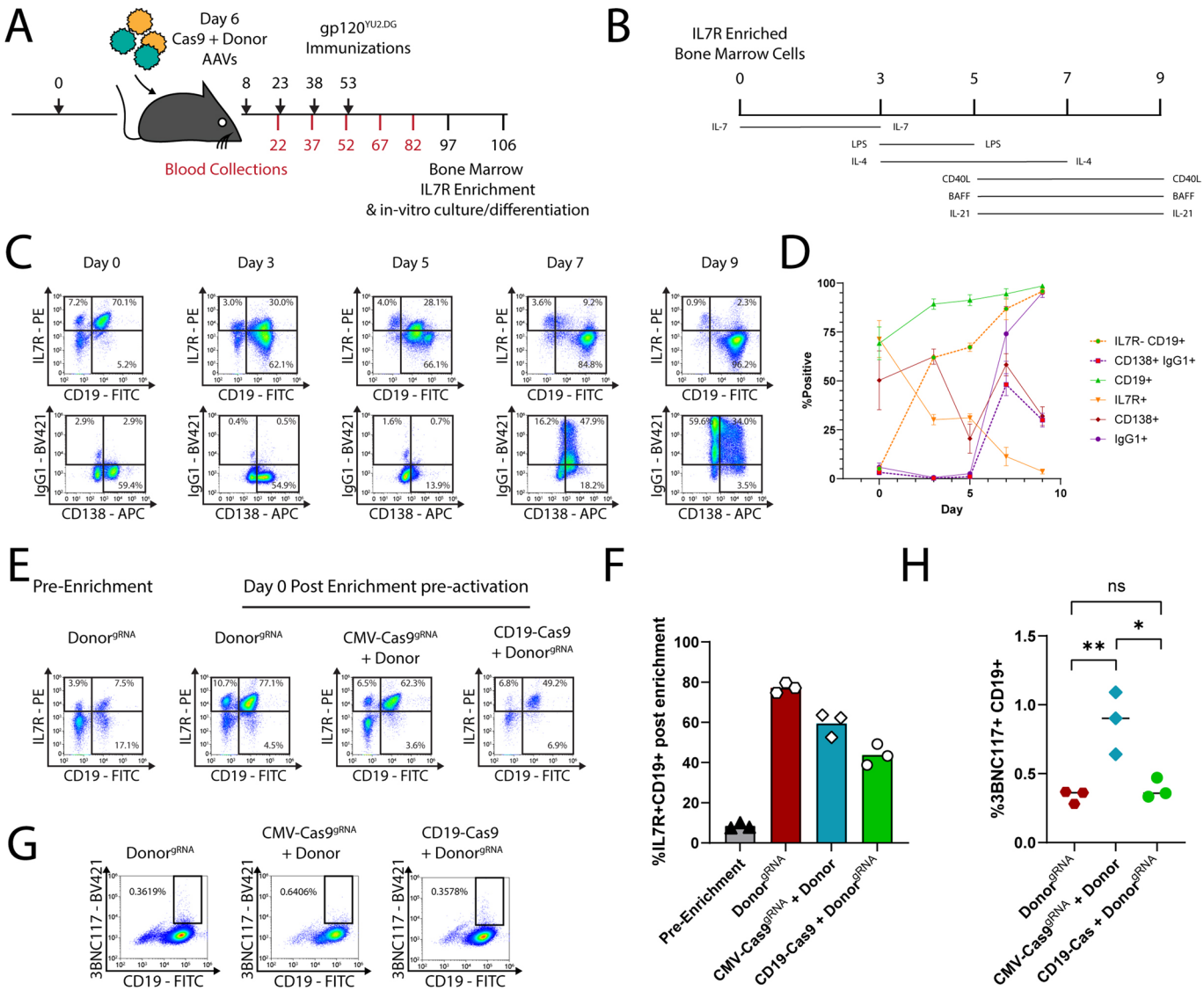

Extended Data Fig. 7 | Using CD19 rather than CMV promoter, to drive saCas9 expression, reduces the engineering rate of B cell progenitors. a. Origin of cells used in this experiment. Bone marrows were extracted 100 days following AAV injection and enriched for IL7R$^+$. **b**. Experimental scheme. Enriched IL7R$^+$ cells were grown in the presence of multiple activation factors as indicated in the representative timeline, numbers indicate days. Horizontal bars below the timeline indicate the presence of a specific factor supplemented to the growth media. **c**. Representative flow cytometry analysis of *in⁻vitro* differentiation of the IL7R$^+$ enriched cells over time. Days as in (B) are indicated above the plots. **d**. Quantification of C. For each group, each line represents n = 3 biologically independent samples. **e**. Representative flow cytometry analysis of IL7R enrichment from mice, as in (A). **f**. Quantification of E. **g**. Representative flow cytometry analysis of 3BNC117$^+$ CD19$^+$ expression by cells, following 9 days of in⁻vitro differentiation, as in (B). **h**. Quantification of G. Each dot represents cells collected from a single mouse as in (A). ns; pv = 0.9, *; pv = 0.0122 and **; pv = 0.0077 for One-Way ANOVA with Tukey's multiple comparison. For C-G, FcR block was used in staining.

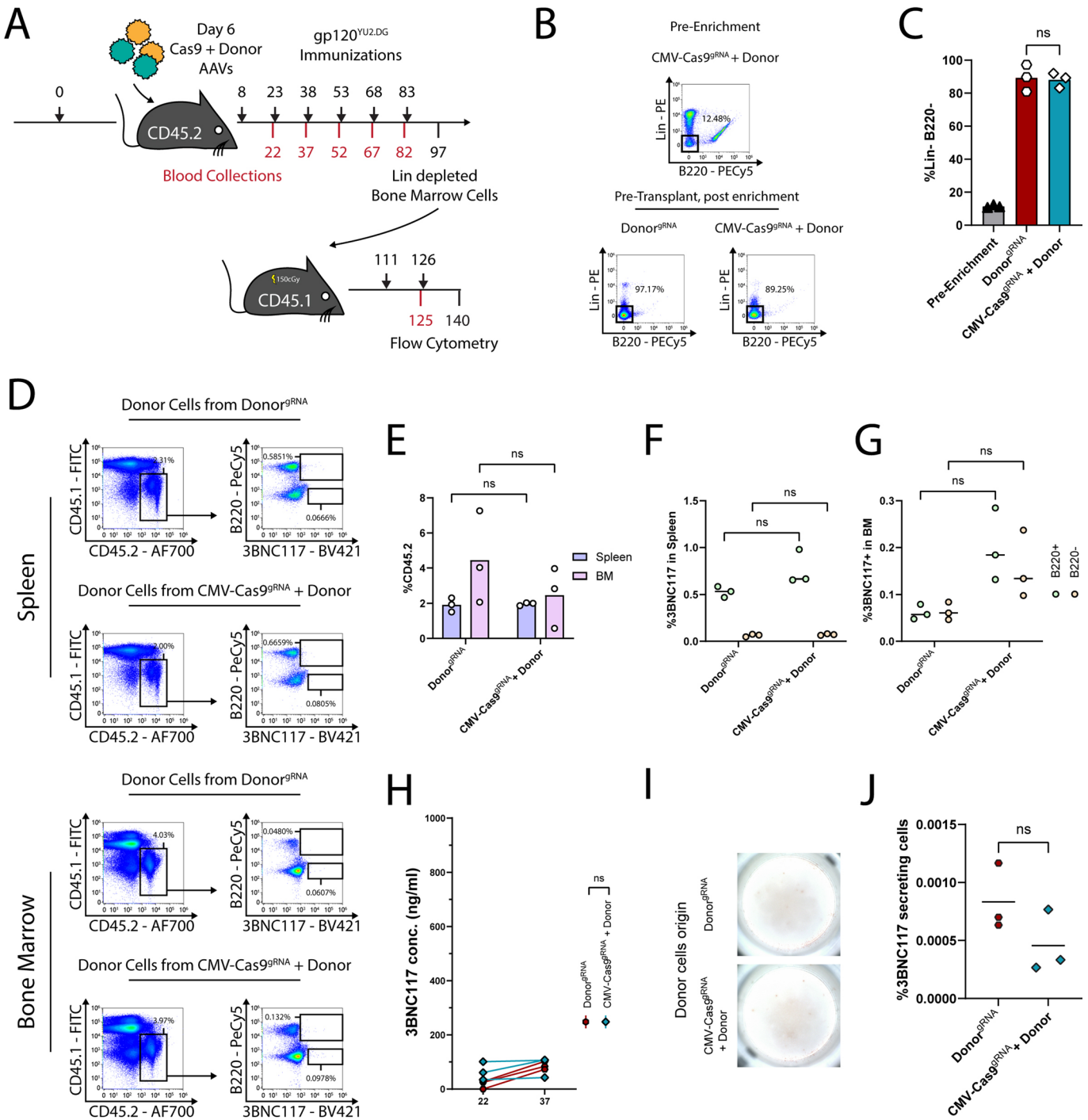

Extended Data Fig. 8 | Low 3BNC117 staining and ELISA levels are obtained following syngeneic transplantation of Lin⁻ enriched cells from mice injected with the donor vector with or without the saCas9 coding vector. a. Experimental scheme. CD45.2 mice received either a donor AAV expressing the gRNA or both a donor AAV and an AAV expressing saCas9 and the gRNA. Immunization protocol is indicated by the bars in black. On day 97, bone marrow cells were collected, enriched for lineage negative cells (Lin⁻) and transplanted into, recipient CD45.1 mice. Recipient mice are sublethally irradiated before transplantation and immunized after transplantation. **b-c**. Representative flow cytometry analysis (B) and quantification (C) of the enriched Lin⁻ population from the donor mice. ns; pv = 0.9627 for One-Way ANOVA with Tukey's multiple comparison. **d**. Representative flow cytometry analysis (D) of spleens (top) or bone marrows (bottom) from recipient mice at day 140, as in (A) **e**. Quantification of D. for the CD45.2⁺ CD45.1⁻ population. From top to bottom: ns; pv = 0.4595 and pv > 0.9999 for Two-Way ANOVA with Tukey's multiple comparison. **f-g**. Quantification of D. for the rate of 3BNC117-expressing cells for the spleen (F) or the bone marrow (G). From top to bottom: ns; pv = 0.9994 and pv = 0.0668 (F) and pv = 0.2371 and pv = 0.0560 for Two-Way ANOVA with Tukey's multiple comparison. **h**. Serum 3BNC117 IgG titers at the indicated time points. The scale of the Y-axis was chosen to correspond to the other 3BNC117 titer plots in this manuscript. ns; pv = 0.1726t for Two-Way ANOVA. **i**. Representative ELISPOT assay of a day 140 bone marrow from CD45.1 recipient mice. **j**. Quantification I. ns; pv = 0.1756 for two-sided unpaired t-test. For B-D, FcR block was used in staining.

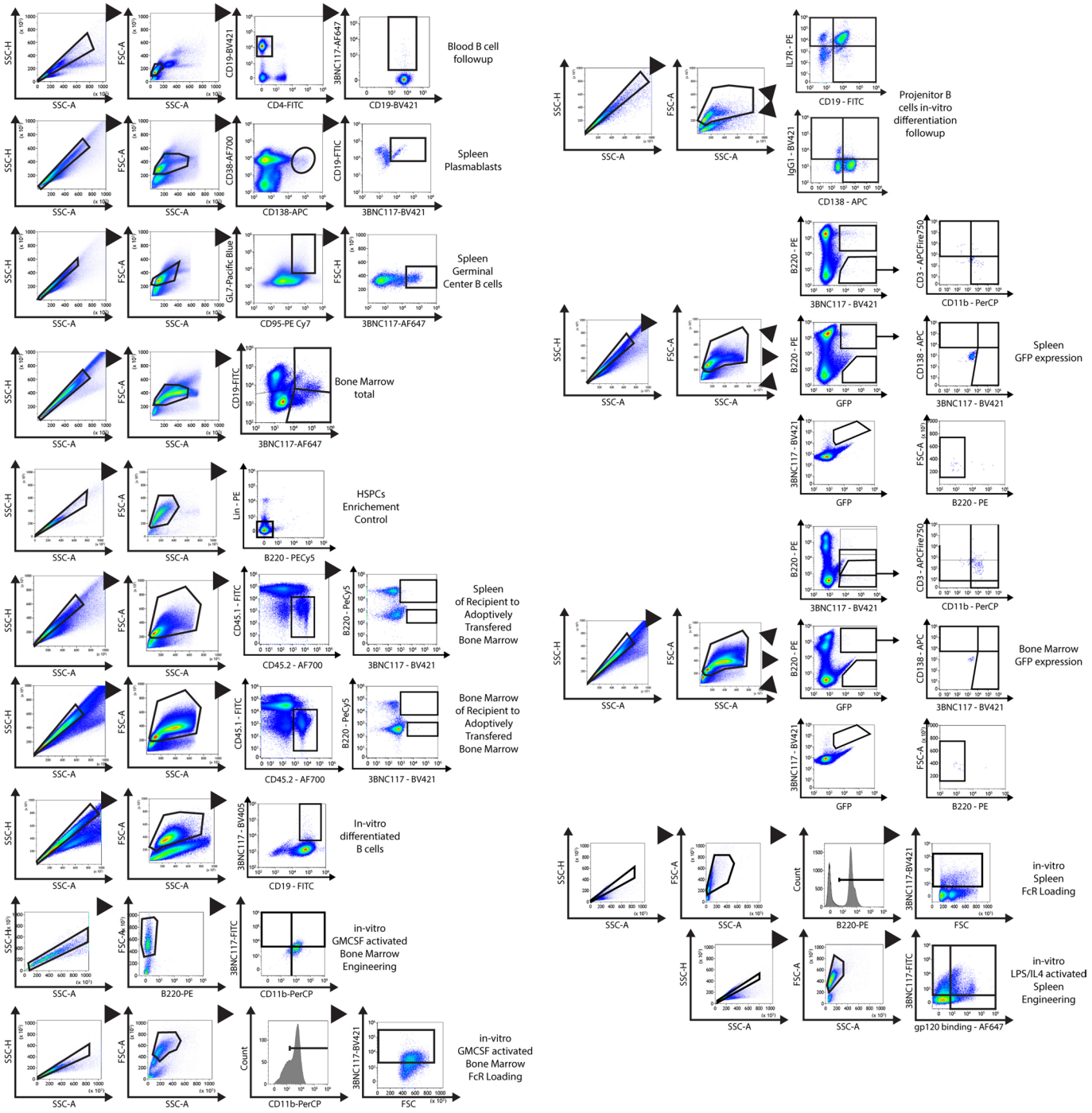

Extended Data Fig. 9 | Gating strategy for each experiment in this study. Gating strategy for each experiment in this study.

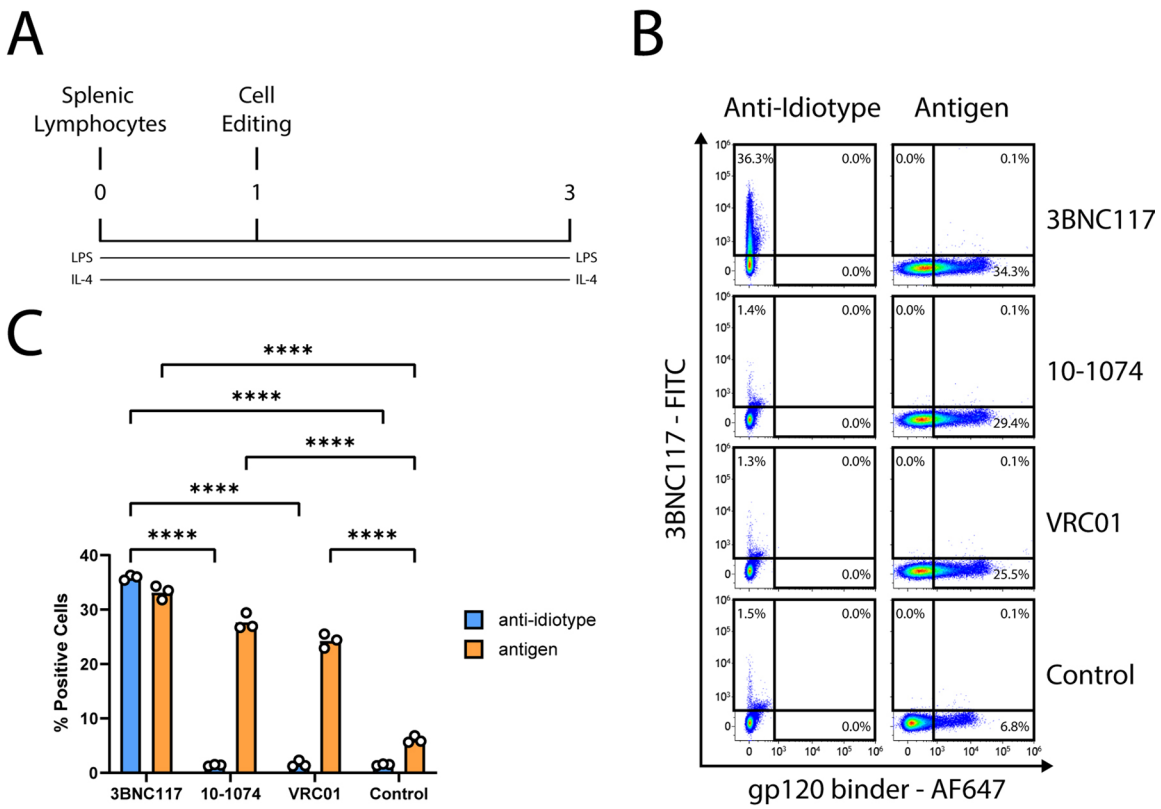

Extended Data Fig. 10 | Assessment of the specificity and sensitivity of the anti-idiotype for 3BNC117. a. Experimental scheme. Cells are engineered a day following extraction from spleen and activation. We used three different donor AAVs, each expressing a different antibody: either 3BNC117, VRC01 or 10−1074. **b**. Flow cytometry of gp120 or anti-idiotype binding of engineered cells, two days following treatment. Staining procedure is indicated above the plots. FcR block was used in staining. Each row indicates a different AAV used. Untransduced cells serve as the negative control. **c**. Quantification of B. ****; pv < 0.0001 for Two-Way ANOVA with Tukey's multiple comparison.

nature research

Corresponding author(s): Adi Barzel

Last updated by author(s): Mar 19, 2022

Reporting Summary

Nature Research wishes to improve the reproducibility of the work that we publish. This form provides structure for consistency and transparency in reporting. For further information on Nature Research policies, see our Editorial Policies and the Editorial Policy Checklist.

Statistics

For all statistical analyses, confirm that the following items are present in the figure legend, table legend, main text, or Methods section.

n/a	Confirmed
☐	☒ The exact sample size (*n*) for each experimental group/condition, given as a discrete number and unit of measurement
☐	☒ A statement on whether measurements were taken from distinct samples or whether the same sample was measured repeatedly
☐	☒ The statistical test(s) used AND whether they are one- or two-sided *Only common tests should be described solely by name; describe more complex techniques in the Methods section.*
☐	☒ A description of all covariates tested
☐	☒ A description of any assumptions or corrections, such as tests of normality and adjustment for multiple comparisons
☐	☒ A full description of the statistical parameters including central tendency (e.g. means) or other basic estimates (e.g. regression coefficient) AND variation (e.g. standard deviation) or associated estimates of uncertainty (e.g. confidence intervals)
☐	☒ For null hypothesis testing, the test statistic (e.g. *F*, *t*, *r*) with confidence intervals, effect sizes, degrees of freedom and *P* value noted *Give P values as exact values whenever suitable.*
☒	☐ For Bayesian analysis, information on the choice of priors and Markov chain Monte Carlo settings
☒	☐ For hierarchical and complex designs, identification of the appropriate level for tests and full reporting of outcomes
☒	☐ Estimates of effect sizes (e.g. Cohen's *d*, Pearson's *r*), indicating how they were calculated

Our web collection on statistics for biologists contains articles on many of the points above.

Software and code

Policy information about availability of computer code

Data collection	Data collection for flow cytometry was performed using CytExpert software v3.2.1 Data collection for Miseq Illumina sequence was performed using Miseq control software v3.1
Data analysis	For Flow cytometry, data analysis was performed using Kaluza Analysis v2.1 (Beckman Coulter) Statistical analysis and data visualization was performed using Prism 8 v8.4.3 or 9 v9.0.1 (GraphPad) Pair-end pairing were performed using Fast Length Adjustment of Short Reads (FLASH) v1.2.11 (https://github.com/ebiggers/flash) On-target CRISPR induced double stranded breaks were analyzed using CRISPRpic v1 (https://github.com/compbio/CRISPRpic) Alignments were performed using Bowtie2 alignment analysis v2.4.2 (https://github.com/BenLangmead/bowtie2) Selection analysis was performed using SELECTON v2.4 (http://selecton.tau.ac.il/) CHANGE-seq analysis was performed using CHANGE-seq analysis software v1.2.9.1 (https://github.com/tsailabSJ/changeseq) CRISPR induced double stranded breaks were compared using TIDE v3.3 (https://tide.nki.nl/) Alignement of Sanger sequencing chromatograms was performed using Snapgene v5.3 and above (GSL Biotech)

For manuscripts utilizing custom algorithms or software that are central to the research but not yet described in published literature, software must be made available to editors and reviewers. We strongly encourage code deposition in a community repository (e.g. GitHub). See the Nature Research guidelines for submitting code & software for further information.

Data

Policy information about availability of data

All manuscripts must include a data availability statement. This statement should provide the following information, where applicable:

- Accession codes, unique identifiers, or web links for publicly available datasets
- A list of figures that have associated raw data
- A description of any restrictions on data availability

Data is available in the main text, in the Supplementary Data and Materials. Illumina sequencing data can be accessed in the SRA database under accession code PRJNA706552. The authors declare that all unique materials used are readily available from the authors upon MTA agreement.

Field-specific reporting

Please select the one below that is the best fit for your research. If you are not sure, read the appropriate sections before making your selection.

☒ Life sciences ☐ Behavioural & social sciences ☐ Ecological, evolutionary & environmental sciences

For a reference copy of the document with all sections, see nature.com/documents/nr-reporting-summary-flat.pdf

Life sciences study design

All studies must disclose on these points even when the disclosure is negative.

Sample size	Due to ethical and financial consideration we used the minimal amount of animals that allowed the derivation of statistically significant conclusions. Thus, cohorts of 3 mice were used as the minimal amount of animals to allow the derivation of statistically significant conclusions. For other experiments, sample size was not predetermined and data was compiled as is.
Data exclusions	No data was excluded
Replication	All attempts for replication were successful. Experiments were replicated or performed independently at least once and up to four times, as described in the figures legends.
Randomization	Mice were allocated randomly into the different experimental groups. For experiments other than those involving mice, samples were allocated randomly.
Blinding	Experiments were not blinded. For off-target CRISPR induced double stranded breaks and somatic hypermutation / clonal selection, analysis was performed independently of experiments. For other experiments ,analysis was performed by the same researchers that conduced the assays.

Reporting for specific materials, systems and methods

We require information from authors about some types of materials, experimental systems and methods used in many studies. Here, indicate whether each material, system or method listed is relevant to your study. If you are not sure if a list item applies to your research, read the appropriate section before selecting a response.

Materials & experimental systems

n/a	Involved in the study
☐	☒ Antibodies
☐	☒ Eukaryotic cell lines
☒	☐ Palaeontology and archaeology
☐	☒ Animals and other organisms
☒	☐ Human research participants
☒	☐ Clinical data
☒	☐ Dual use research of concern

Methods

n/a	Involved in the study
☒	☐ ChIP-seq
☐	☒ Flow cytometry
☒	☐ MRI-based neuroimaging

Antibodies

Antibodies used	HRP conjugated anti-mouse IgM (Jackson Immunoresearch, 715-035-140) HRP conjugated anti-mouse IgG (Jackson Immunoresearch, 715-035-151) HRP conjugated anti-mouse IgG1 (Jackson Immunoresearch, 715-035-205) HRP conjugated anti-mouse IgA (SouthernBiotech 1040-05) HRP conjugated anti-mouse IgG2c (BioRad, STAR-135P) FITC labeled anti-mouse CD19 (Biolegend, 152403) BV421 labeled anti-mouse CD19 (Biolegend, 115538)

APC labeled anti-mouse CD138 (Biolegend, 142506)
Pacific Blue labeled anti mouse GL7 antigen (Biolegend, 144613)
PE-Cy7 labeled anti-mouse CD95 (BD Bioscience, 557653)
AF700 labeled anti-mouse CD38 (eBioscience, 56-0381-82)
BV421 labeled anti-human IgK (Biolegend, 392705)
AF647 labeled anti-human IgG1 (Abcam, ab200623)
Anti-idiotypic 3BNC117 (produced in-house)
Anti-mouse CD16/32 (TruStain FcX) (Biolegend, 156603),
Anti-mouse/human CD11b (Biolegend, 101229),
Anti-mouse CD3 (Biolegend, 100247),
Anti-mouse/human CD45R/B220 (Biolegend, 103208),
Anti-mouse/human CD45R/B220 (Biolegend, 103210),
Anti-mouse CD127/IL7R (Miltenyi Biotec, 130-125-101),
Anti-mouse IgG1 (BD Bioscience, 562580),
Anti-mouse CD45.1 (invitrogen, 11-0453-85),
Anti-mouse CD45.2 (invitrogen, 56-0454-81),
Anti-mouse Lineage cocktail (Biolegend, 78035),
Anti-human IgG Fc (Biolegend, 410719),
Anti-6 His epitope Tag (Biolegend, 906116)

Validation

All BD Bioscience antibodies listed are tested by the manufacturer for flow cytometry on murine cells.
Murine targeting Biolegend antibodies listed are tested by the manufacturer for flow cytometry on murine cells.
Human targeting Biolegend antibodies listed are tested by the manufacturer for flow cytometry on human cells.
All invitrogen antibodies are tested by the manufacturer for flow cytometry on mouse splenocyte suspensions.
The Miltenyi Biotec antibody is tested by the manufacturer for flow cytometry on mouse splenocytes.
Southern Biotech antibodies listed are tested by the manufacturer for flow cytometry and ELISA with known reactivity to mouse.
All Jackson Immunoresearch antibodies were reported to work with ELISA on murine samples.
All BioRad antibodies listed are tested by the manufacturer for ELISA and flow cytometry on murine samples.
All abcam antibodies listed are tested by the manufacturer for ELISA and flow cytometry on murine samples.
In house produced antibodies were tested for flow cytometry and ELISA and have specificity for the idiotype of 3BNC117 with data provided in this manuscript and in Nahmad et al. 2020, Nature Communications.
eBioscience antibodies are tested by the manufacturer for flow cytometry, on mouse splenocytes

Eukaryotic cell lines

Policy information about cell lines

Cell line source(s)

Expi293F cell line (ThermoFisher, A14635) was provided by the Wine lab, Tel Aviv University. 293t cells (ATCC CRL-3216) were provided commercially.

Authentication

293t cells were commonly identified by flow cytometry during study-unrelated experiments in the lab
Expi293F cells were commonly identified by microscopy during routine checks

Mycoplasma contamination

Cell lines tested negative for mycoplasma contamination during routine checks

Commonly misidentified lines
(See ICLAC register)

No commonly misidentified cell lines were used.

Animals and other organisms

Policy information about studies involving animals; ARRIVE guidelines recommended for reporting animal research

Laboratory animals

6-9 weeks old female CD45.2 C57BL/6OlaHsd mice (Envigo), housed in standard animal facility conditions as regulated by the Tel Aviv University Animal Facility. CD45.1 C57BL/6OlhaHsd mice were provided by the Lapidot lab, Weizmann Institute of Science and were also housed in standard animal facility conditions as regulated by the Tel Aviv University Animal Facility

Wild animals

The study did not involve wild animals

Field-collected samples

The study did not involve samples collected from the field

Ethics oversight

All mouse experiments were done with approval of Tel Aviv University ethical committees

Note that full information on the approval of the study protocol must also be provided in the manuscript.

Flow Cytometry

Plots

Confirm that:

☒ The axis labels state the marker and fluorochrome used (e.g. CD4-FITC).

☒ The axis scales are clearly visible. Include numbers along axes only for bottom left plot of group (a 'group' is an analysis of identical markers).

☒ All plots are contour plots with outliers or pseudocolor plots.

☒ A numerical value for number of cells or percentage (with statistics) is provided.

Methodology

Sample preparation	Blood samples from mice were collected in heparin. Cells and serum were separated by centrifugation. For spleens, whole spleens were extracted from mice and mechanically crushed in PBS to be filtered in a 70 µm cell strainer (Corning). For bone marrow, cells were flushed from the posterior femur and tibia. For blood, spleen and bone marrow, cells were processed with red blood cell lysis buffer (Biolegend) and plated in 1640 RPMI (Biological Industries) supplemented with 10% HI FBS (Biological Industries) until processing, 30min-1hour following extraction. Harvested cells from spleen, bone marrow or blood were resuspended in cell staining buffer (Biolegend) and incubated with 2µg/100µl of human anti-3BNC117 and, were relevant, 1µg/100µl of Anti-mouse CD16/32 (TruStain FcX, Biolegend) for 10 mins, washed and resuspended again in cell staining buffer containing secondary antibodies. Secondary staining was performed in the dark, for 15 mins. Cells were washed and resuspended in staining buffer before reading in an a CytoFLEX (Beckman Coulter), Attune NxT (life Technologies) flow cytometers or BD AriaIII (BD Biosciences) FACS.
Instrument	CytoFLEX (Beckman Coulter) or Attune Nxt (life Technologies) or BD AriaIII (BD Biosciences)
Software	Kaluza (Beckman Coulter)
Cell population abundance	1000-5000 cells were sorted for engineered B cells (3BNC117+, CD4-, CD19+) phenotype on a FACS BD AriaIII (BD Biosciences). RNA was extracted directly, in bulk, following sorting. No assessment for purity was performed.
Gating strategy	The gating strategy is detailed in the legend of each panel and depicted in figure S13

☒ Tick this box to confirm that a figure exemplifying the gating strategy is provided in the Supplementary Information.